THE UNIVERSITY OF ALBERTA

THE DRIFT INSTABILITY IN THE PRESENCE OF NONUNIFORM ELECTRIC AND DIAMAGNETIC ROTATIONS

by

© MALCOLM CAPLAN

A THESIS

SUBMITTED TO THE FACULTY OF GRADUATE STUDIES

IN PARTIAL FULFILMENT OF THE REQUIREMENTS FOR THE DEGREE

OF MASTER OF SCIENCE

DEPARTMENT OF ELECTRICAL ENGINEERING

EDMONTON, ALBERTA

FALL, 1971

UNIVERSITY OF ALBERTA

FACULTY OF GRADUATE STUDIES

The undersigned certify that they have read, and recommend to the Faculty of Graduate Studies for acceptance, a thesis entitled "The Drift Instability in the Presence of Nonuniform Electric and Diamagnetic Rotations", submitted by Malcolm Caplan in partial fulfilment of the requirements for the degree of Master of Science.

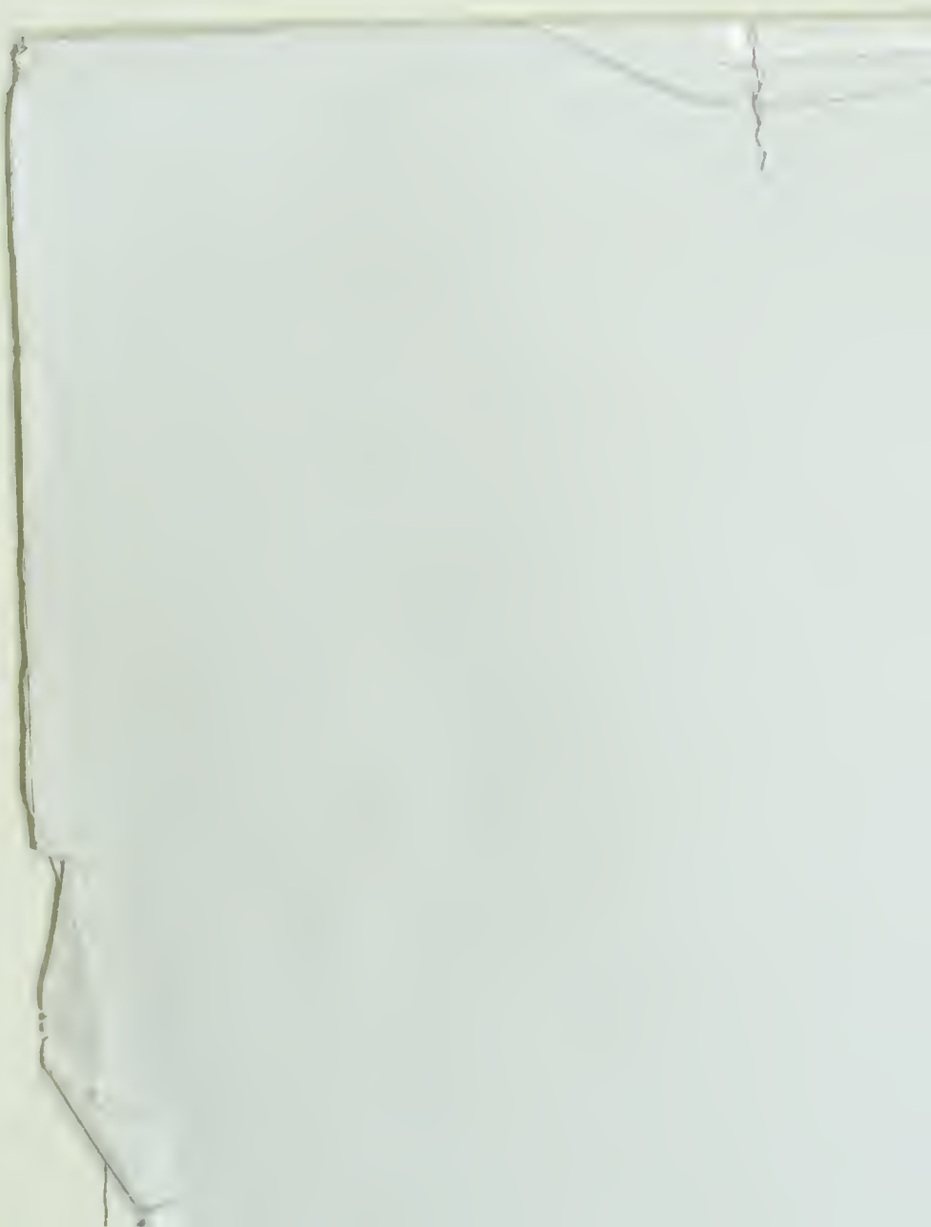

ABSTRACT

The collisionless drift wave, with a component of the propagation vector parallel to the magnetic field, is examined in a nonuniformly rotating cylindrical plasma. Terms involving the ratio of the Alfvén velocity (C_A) to the velocity of light (C) are retained in the analysis allowing plasmas in different density regimes to be investigated. The differential equation describing the drift mode is solved numerically. Approximate analytic solutions are also given using the WKB method and a Weber-Hermite approximation.

It is found that the velocity shear resulting from nonuniform electric and diamagnetic rotations can provide the dominant contribution to the growth rate of the wave. The destabilizing effect of nonuniform rotations is further enhanced in lower density plasmas where terms involving $(C_A/C)^2$ are no longer negligible.

ACKNOWLEDGEMENTS

The author wishes to express his thanks to Dr. C.E. Capjack and Dr. C.R. James who supervised this project. The many valuable discussions and suggestions greatly contributed to the completion of this thesis.

The author also wishes to thank the National Research Council of Canada and the Department of Electrical Engineering, University of Alberta, for financial support during this work.

Acknowledgement is also extended to the author's mother for her assistance in typing the manuscript and to his wife for her support.

TABLE OF CONTENTS

LIST OF SYMBOLS

n_o^e	equilibrium electron density
n_o^i	equilibrium ion density
n_1^i	perturbed ion density
n_1^e	perturbed electron density
a_i	ion Larmor radius
a_e	electron Larmor radius
Ω_i	ion cyclotron frequency
Ω_e	electron cyclotron frequency
V_{TH}^i	ion thermal velocity
V_{TH}^e	electron thermal velocity
W_E	electric angular frequency
W_{EN}	electron diamagnetic frequency
$W_\wedge$	ion diagmagnetic frequency
M_e	electron mass
M_i	ion mass
B	magnetic field
T	temperature of ions and electrons
k	Boltzmann's constant
e	electron charge

$K_{\shortparallel}$	parallel wave number
ϕ	equilibrium electric potential
ϕ_1	perturbed electric potential
m	azimuthal wave number
W	complex wave frequency
W_R	wave frequency
W_I	growth rate (imaginary part of W)
W_o	"doppler-shifted" complex wave frequency $(W-mW_E)$
W_R^o	"doppler-shifted" wave frequency (W_R-mC_E)
L_N	density scale length
L_E	electric scale length
r_M	radius at peak electric and diamagnetic rotations
C_{NE}	peak diamagnetic rotation
C_E	peak electric rotation
b	parameter representing the non-uniformity in the diamagnetic rotation
r_p	plasma radius
C_A	Alfvén velocity
C	velocity of light
ψ	perturbed guiding centre displacement
f_o	equilibrium distribution function
$\vec{V}_{PH}$	phase velocity of the wave
V_{PH}^z	phase velocity in the axial direction

CHAPTER I

INTRODUCTION

Many phenomena which occur in a confined laboratory plasma cannot be adequately described by using the infinite homogeneous model. The effects of temperature gradients, density gradients, finite lengths, boundary conditions and external field configurations become significant in the laboratory and thus can produce a whole new host of waves and instabilities. It is worthwhile digressing for a moment as to the exact meaning of an instability. Since the Hamiltonian of a plasma does not contain magnetic field terms, a plasma confined by a magnetic field must be in a state of non-equilibrium. This is because the only equilibrium distribution is a Maxwellian, which is a function only of the Hamiltonian. Thus instabilities produced within a plasma are really the result of the plasma trying to approach an equilibrium configuration independent of any magnetic fields. One mechanism for attaining equilibrium is through binary collisions. However there are mechanisms by which collisionless plasmas (collision frequency is small compared to wave frequency) can approach equilibrium. It is this latter type of instability which will be of concern here.

Instabilities can be divided into two types: hydromagnetic instabilities and microinstabilities. Hydromagnetic instabilities are those derived from the fluid equations where essentially the magnetic field lines are "frozen" into the plasma as a result of the constancy of flux through a material surface moving with the fluid. These

instabilities are large scale, rapid and chaotic, moving the plasma as a whole away from a confined configuration. The microinstabilities however can only be derived from microscopic equations such as the Boltzmann equation. These instabilities develop from small perturbations within the plasma which grow with time. The resulting turbulence and diffusion ultimately destroy the confinement of the plasma. Only small groups of particles may be initially involved with microinstabilities as compared to the whole plasma in the hydromagnetic case.

One of the important microinstabilities which has been investigated is the collisionless drift wave (Krall[1], Rosenbluth[2], Politzer[3]) which arises as a result of the density gradients inherent in any confined plasma. The wave, which is driven by a resonant particle interaction is shown to be characterized by a low frequency (1-10 KHz) and a small growth rate. It was found that in many plasma devices non-uniform electric fields were present which resulted in a non-uniform rotation of the plasma. Deviations from a gaussian density profile also resulted in non-uniform rotations. The paper by Capjack and Stringer[4] investigated the effects of non-uniform rotations on the drift wave when the density was sufficiently high so that terms involving the ratio of the Alfvén velocity to the velocity of light could be ignored. Numerical studies were made showing the dependence of the growth rate and frequency of the drift wave on the magnitudes and scale lengths of the electric fields and density gradients present.

The purpose of this thesis will be first to provide some back-

ground on the drift mode and the experimental conditions under which it can be observed. A brief explanation for the steady state electric fields found in some plasma devices will be given. The drift mode will then be examined in a non-uniformly rotating cylindrical plasma. Terms involving the ratio of the Alfvén velocity to the velocity of light will be retained in the differential equation describing the drift mode. This will allow lower density plasmas to be investigated. Approximate analytic solutions both qualitative and quantitative in nature will be given using the WKB method and a Weber-Hermite approximation. The analytical results will help clarify the numerical results presented and will illustrate the physical mechanisms involved. Conclusions will be drawn concerning the effects of non-uniform electric fields and density gradients on the drift instability for density regimes typical of many plasma devices.

CHAPTER II

THE DRIFT INSTABILITY

2.1 Physical Mechanism

Following the methods of Davidson and Kammash,[5] Stringer,[6] Meade[7] and Sagdeev,[8] a heuristic derivation of the frequency and growth rate of the drift wave will be given.

A plasma, if it is to be in equilibrium according to the fluid model, must exhibit diamagnetism. From the Navier-Stokes equation for ions or electrons in equilibrium one has:

$$\vec{J} \times \vec{B} = \nabla P = \nabla nkT \qquad (2.1)$$

where $\vec{J}$ = current density = $ne\vec{V}$

$\vec{B}$ = magnetic field

n = density

T = temperature

P = pressure

$\vec{V}$ = macroscopic velocity

e = charge

k = Boltzmann's constant

For a cylindrical geometry where the density gradient is in the radial direction and a uniform magnetic field is in the axial direction, equation (2.1) yields:

$$\vec{V}_d^e = \frac{-kT}{eB}\frac{n^e(r)'}{n^e(r)}\hat{\varepsilon}_\theta \qquad \vec{V}_d^i = \frac{-kT}{eB}\frac{n^i(r)'}{n^i(r)}\hat{\varepsilon}_\theta \tag{2.2}$$

where

$\vec{V}_d^e$ = electron diamagnetic drift velocity in the azimuthal direction ($\hat{\varepsilon}_\theta$)

$\vec{V}_d^i$ = ion diamagnetic drift velocity in the azimuthal direction

$'$ denotes differentiation with respect to r

i,e denotes ions or electrons respectively

The electrons and ions thus have diamagnetic drift velocities given by equation (2.2) which provide currents necessary for hydrodynamic equilibrium. By using a simple model requiring charge neutrality when ions move across the field lines with an electric drift velocity and electrons adjust their density according to a Maxwellian, it can be shown that a wave may exist propagating in the electron diamagnetic drift direction with a phase velocity (V_{PH}) equal to that of the electron diamagnetic drift velocity. Ion motion in the axial direction is neglected since it will be shown later that a drift wave will locate itself in a region where the ion thermal velocity is much less than the phase velocity of the wave.

One begins by considering an inhomogeneous neutral plasma in a

uniform axial magnetic field with a density gradient in the radial direction. An electrostatic wave perturbation (normal mode) is assumed to develop with a wave vector $\vec{K}$ in the axial and azimuthal direction (Figure 1).

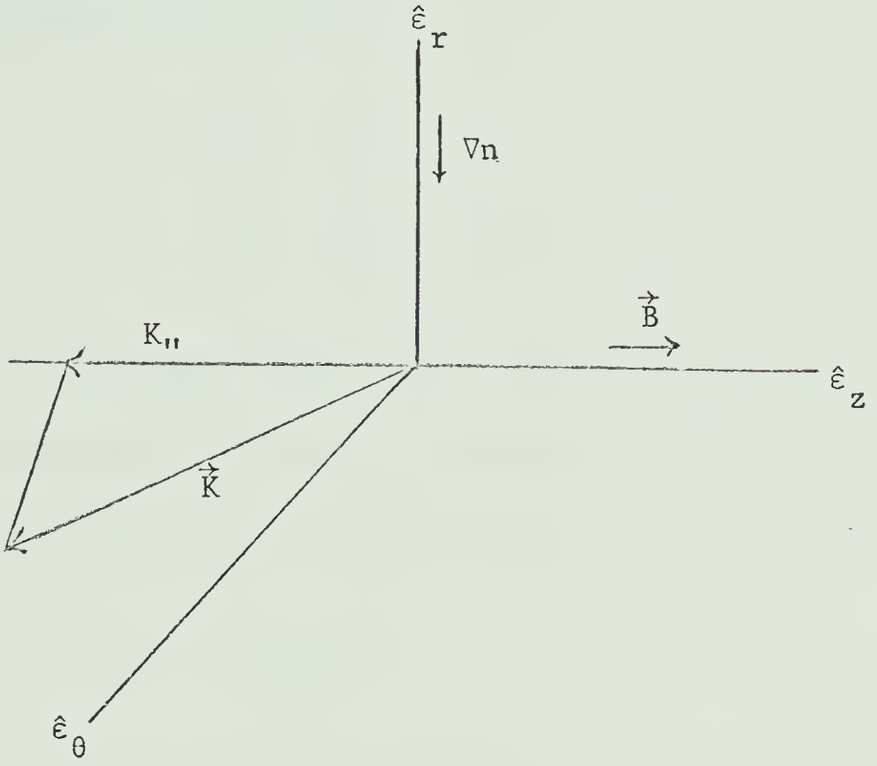

Figure 1 - Simple plasma model in a local co-ordinate system

The perturbed potential is of the form:

$$\phi_1 = \exp\left[i(m\theta + K_{\parallel}z - Wt)\right] \tag{2.3}$$

where $K_{\parallel}$ and m are the wave numbers in the $\hat{\varepsilon}_z$ and $\hat{\varepsilon}_\theta$ directions respectively. The electric field corresponding to ϕ_1 is given by:

$$\vec{E} = -\nabla\phi_1 = -K_{\parallel}\phi_1\hat{\varepsilon}_z - \frac{im\phi_1}{r}\hat{\varepsilon}_\theta \tag{2.4}$$

The equation of continuity for ions is:

$$\frac{\partial n^i}{\partial t} + \nabla \cdot (n^i \vec{V}^i) = 0 \qquad (2.5)$$

which is linearized by letting

$$n^i = n_o^i + n_1^i$$

$$\vec{V}^i = \vec{V}_o^i + \vec{V}_1^i \simeq \vec{V}_1^i \quad \text{(since the ions are cold)}$$

where $\vec{V}_1^i$ is the first order $\vec{E}$ X $\vec{B}$ drift velocity in the radial direction resulting from the perturbation ϕ_1. The continuity equation then gives an expression for the perturbed ion density n_1^i:

$$n_1^i = \frac{-m}{r} \frac{\phi_1}{BW} n_o^{i'} \qquad (2.6)$$

With the flow of electrons not limited in any way, they are locally Maxwellian along the perturbation and so the perturbed electron density is:

$$n_1^e = n_o^e \frac{e\phi_1}{kT} \qquad (2.7)$$

By using the quasi-neutrality condition ($n^e \simeq n^i$), which is valid for sufficiently high density, it can be established that the dispersion relation is:

$$W = \frac{-mkT}{eB} \frac{n_o^{e'}}{n_o^e r} = mW_{EN} \qquad (2.8)$$

where

$$W_{EN} = \frac{-kT}{eB} \frac{n_o^{e'}}{n_o^e r} = \text{the electron diamagnetic angular drift velocity } (V_d^e / r)$$

From this simple model, the drift wave is seen to be neutrally stable (imaginary W = 0) having an angular frequency equal to a multiple m times the electron diamagnetic angular frequency (W_{EN}). Since this model neglects microscopic effects by ignoring the finite velocity spread of the particles, it cannot correctly predict the growth rate of the wave. There are mechanisms limiting the flow of neutralizing current along the field lines resulting in an exchange of energy between the wave and the particles. These mechanisms take the form of collisional resistance for a collisional plasma and resonant particle effects for a collisionless plasma. The result is a positive imaginary part of W giving rise to a growing unstable wave. The following argument (Meade[7]) gives an estimate for the growth rate in a collisionless plasma.

A wave will grow in a plasma when particles transfer energy to the wave. One can look at the particle wave interaction as being composed of two types of interactions. One interaction results from particles travelling slightly faster or slower than the phase velocity of the wave. This gives rise to Landau damping (Stix[9]). The other interaction results from particles travelling exactly at the phase velocity

of the wave. In this case particles can either give energy to the wave or take energy from the wave, depending on the direction of wave propagation and sign of the charged particles. The physical mechanism for this second type of interaction is now given.

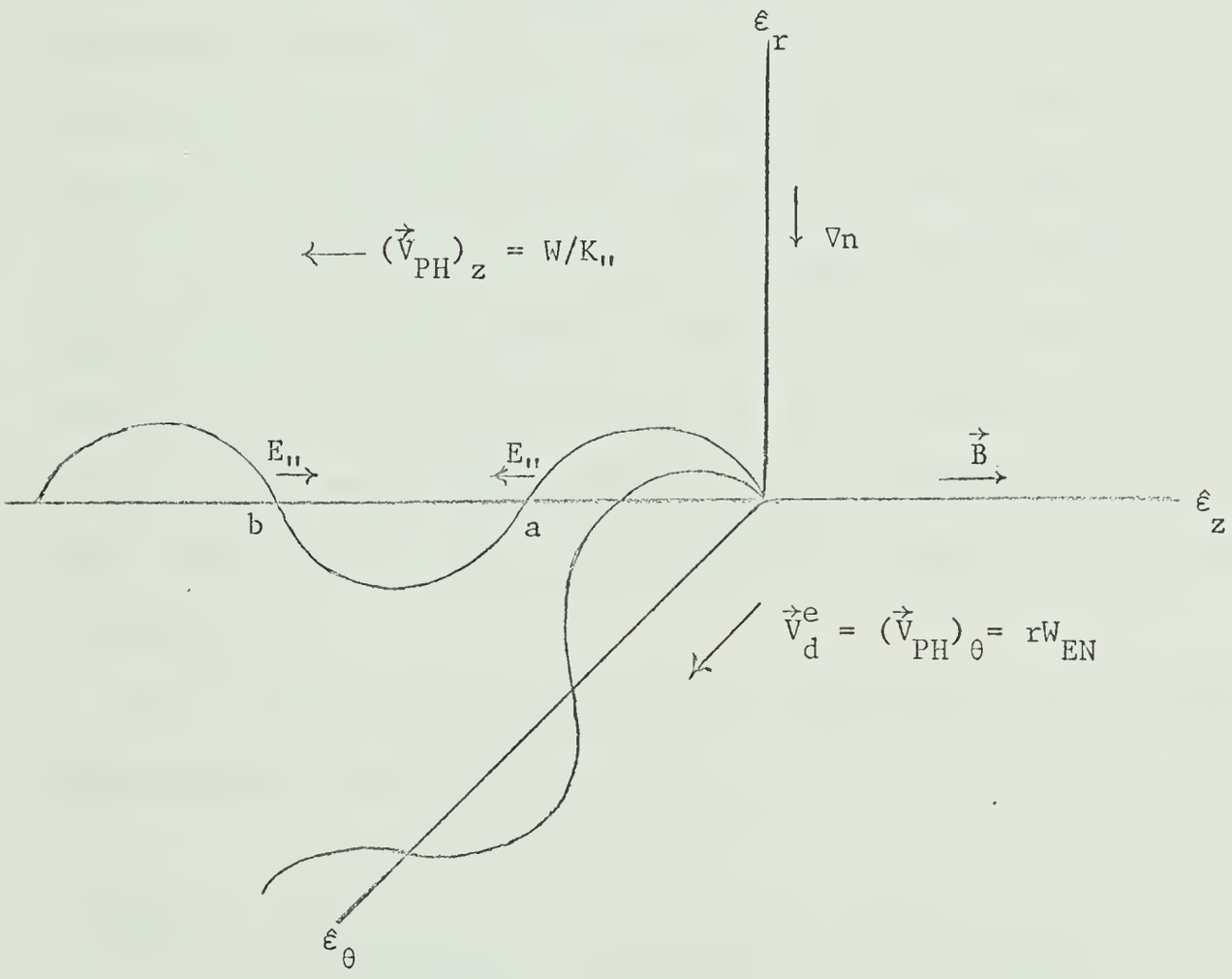

Figure 2 - Equi-potential surfaces of a collisionless drift wave in a local co-ordinate system in cylindrical geometry

Figure 2 shows a drift wave whose phase velocity in the azimuthal direction is the same as the electron diamagnetic drift velocity. The streaming ions or electrons along the magnetic field lines interact with the z-component of $\vec{E}(E_{\parallel})$. For the moment, electrons only are considered. At position "a" resonant electrons experience a constant $\vec{E} \times \vec{B}$ drift in the radial direction. At position "b" resonant electrons experience the $\vec{E} \times \vec{B}$ drift in the opposite direction. The direction in which resonant electrons travel is such that the electron current at "a" opposes $E_{\parallel}$ giving energy to the wave while the current at "b" is in the same direction as $E_{\parallel}$ taking energy from the wave. Because of the density gradient, there will be more electrons at "a" than at "b" and thus the net result is that resonant electrons give energy to the wave. Since the ions are of opposite charge, they will take energy from the wave. The quantitative aspects of the above are now given.

The net power per cycle delivered to the wave by the resonant electrons and ions is shown to be[7]:

$$-(\vec{J}\cdot\vec{E})_R = \sqrt{\pi}\left(\frac{E_{\parallel}^2}{8\pi}\right)\left(\frac{8\pi ne^2}{2kTK_{\parallel}^2}\right)\left\{\left(\frac{W}{K_{\parallel}V_{TH}^e}\right)(mW_{EN})\ \exp\left[-\left(\frac{W}{K_{\parallel}V_{TH}^e}\right)^2\right]\right.$$

$$\left. - \left(\frac{W}{K_{\parallel}V_{TH}^i}\right)(mW_{EN})\ \exp\left[-\left(\frac{W}{K_{\parallel}V_{TH}^i}\right)\right]\right\} \qquad (2.9)$$

where the assumptions made are that:

i. The velocities of the ions and electrons in the axial direction follow Maxwellian distributions which are at the same temperature T.

ii. The phase velocity of the wave in the axial direction $(W/K_{\shortparallel})$ is much less than the ion thermal velocity (V_{TH}^{i}) or the electron thermal velocity (V_{TH}^{e})

iii. The electron and ion densities are approximately equal $(n^{i} \simeq n^{e} = n)$

The net power per cycle taken from the wave by electron and ion Landau damping is given by[9]:

$$(\vec{J}\cdot\vec{E})_{L} = \sqrt{\pi}\left(\frac{E_{\shortparallel}^{2}}{8\pi}\right)\left(\frac{8\pi ne^{2}}{2kTK_{\shortparallel}^{2}}\right)\left\{\left(\frac{W}{K_{\shortparallel}V_{TH}^{e}}\right)(W)\ \exp\left[-\left(\frac{W}{K_{\shortparallel}V_{TH}^{e}}\right)^{2}\right]\right.$$

$$\left. + \left(\frac{W}{K_{\shortparallel}V_{TH}^{i}}\right)(W)\ \exp\left[-\left(\frac{W}{K_{\shortparallel}V_{TH}^{i}}\right)^{2}\right]\right\} \qquad (2.10)$$

where the same assumptions are made as for (2.9).

The energy per unit volume in the drift wave is given by:

$$\frac{(\varepsilon\cdot\vec{E})\cdot\vec{E}}{8\pi} \simeq \left(\frac{E_{z}^{2}}{8\pi}\right)\left(\frac{8\pi ne^{2}}{2kTK_{\shortparallel}^{2}}\right) \qquad (\varepsilon = \text{dielectric tensor} \qquad (2.11)$$

where the assumptions made in addition to those of equation (2.9) are:

i. the wave frequency W is much less than the ion cyclotron frequency (Ω_i)

ii. the ion Larmor radius (a_i) is much less than r/m

Since $\vec{E}$ varies as $\exp(-iWt) = \exp(iW_R t)\exp(W_I t)$ where W_R is the real part of W and W_I is the imaginary part of W, the equation for the conservation of energy is:

$$\frac{2W_I(\varepsilon\cdot\vec{E})\cdot\vec{E}}{8\pi} = -\left[(\vec{J}\cdot\vec{E})_R + (\vec{J}\cdot\vec{E})_L\right] \tag{2.12}$$

When equations (2.9), (2.10) and (2.11) are substituted into (2.12) the expression for the growth rate W_I becomes:

$$W_I = \sqrt{\pi}(W_{EN} - W)\left(\frac{W}{K_{\parallel}V_{TH}^e}\right)\exp\left[-\left(\frac{W}{K_{\parallel}V_{TH}^e}\right)^2\right]$$

$$-\sqrt{\pi}(W_{EN} + W)\left(\frac{W}{K_{\parallel}V_{TH}^i}\right)\exp\left[-\left(\frac{W}{K_{\parallel}V_{TH}^i}\right)^2\right] \tag{2.13}$$

It can be seen from (2.13) that if ion Landau damping is allowed ($W/K_{\parallel}V_{TH}^i << 1$) the drift mode with $W_R \simeq mW_{EN}$ will be highly damped (since $V_{TH}^i << V_{TH}^e$). If the drift mode is in a region where ion Landau damping does not occur ($W/K_{\parallel}V_{TH}^i >> 1$) the growth rate becomes:

$$W_I = \sqrt{\pi}(mW_{EN} - W)\left(\frac{W}{K_{\parallel}V_{TH}^{e}}\right)\exp\left[-\left(\frac{W}{K_{\parallel}V_{TH}^{e}}\right)^2\right] \qquad (2.14)$$

One can see that in this case there is a competition between the process of electron Landau damping, which causes the wave to damp, and resonant particle interaction which causes the wave to grow. By using the fluid model it was found that $W = mW_{EN}$; it might be concluded that the wave is neutrally stable since the two interaction processes balance each other. It is thus evident that any effect which causes $W < W_{EN}$ will give rise to an instability in the region where ion Landau damping can be ignored. In chapter three it will be shown that the finite Larmor radius of the ions allows $W < W_{EN}$.

One can interpret the physical mechanism of the drift mode in a slightly different manner (Stringer,[6] Sagdeev[8]) which shows the two types of interactions mentioned above really to be manifestations of the same basic Landau interaction. The Landau theory shows that if the number of particles moving slightly slower than the phase velocity of the wave exceeds the number moving slightly faster, the plasma will be stable against self-excitation. For a homogeneous plasma this condition becomes $\partial f_o/\partial V_z\big|_{V_z=V_{PH}^{z}} < 0$ which is satisfied for a Maxwellian distribution. (f_o is the equilibrium distribution function, V_{PH}^{z} is the phase velocity in the axial direction and V_z is the particle velocity in the axial direction.)

However, in an inhomogeneous plasma, terms involving ∇f_o occur in the Vlasov equation (Appendix A). The stability criteria then becomes $\left[\partial f_o/\partial V_z - (m/r)(V_z/W\Omega_e)\partial f_o/\partial r \right]\Big|_{V_z=V_{PH}^z} < 0$. The term $-(m/r)(V_z/W\Omega_e)\partial f_o/\partial r$ is positive for a wave propagating in the electron diamagnetic drift direction. If the plasma has a Maxwellian distribution where the thermal velocity of the particles is much greater than the phase velocity of the wave, the term $\partial f_o/\partial V_z$ will be a small negative quantity and thus the stability criteria can be violated. What has happened is that the density gradient has upset the number of particles going slightly slower or faster than the wave. Resonant particles are brought in from regions of different densities distorting the velocity distribution. The number of particles going slightly faster than the wave then exceeds the number going slightly slower giving rise to instability.

The following conclusions can now be drawn concerning the drift mode:

i. The drift wave occurs in a frequency range such that $V_{TH}^i << V_{PH}^z << V_{TH}^e$. The inequality $V_{PH}^z >> V_{TH}^i$ is necessary to avoid ion Landau damping which will tend to stabilize the wave. The inequality $V_{PH}^z << V_{TH}^e$ is necessary so that the density gradient can distort the distribution function sufficiently to allow the number of particles moving faster than the wave to exceed the number moving slower.

ii. Any effect which allows the wave frequency to be less than the electron diamagnetic frequency will give rise to instability.

iii. The growth rate W_I is much less than the frequency W_R (equations (2.8), (2.13)

2.2 Experimental Conditions

Experimental identifications of the drift mode[3,10] have been successful in devices known as "Q-machines". A typical "Q-machine" consists of a cylindrical vacuum approximately 100 centimetres long and 5 centimetres in diameter in which a uniform axial magnetic field of about 2000 to 5000 Gauss is produced. At each end of the cylinder are tungsten hotplates heated to temperatures of about 2000 degrees Kelvin by electron bombardment from a hot filament. One plate is usually free to move so that the axial length of the machine can be varied. The plasma is produced thermionically by spraying a beam of neutral lithium or sodium atoms into the hot-plates. The beam then becomes ionized. Thermoelectric emission of electrons from the hot plates provide the charge necessary to keep the plasma "quasi-neutral". Due to the random nature in the method of plasma production, it is assumed that the electron and ion velocity distributions in the axial direction are Maxwellians

having a temperature equal to that of the hotplate. Typical particle densities are of the order $10^8/cm^3$ which puts the plasma in a collisionless regime since the mean free path is several machine lengths.

Two important aspects in "Q-machines" are the density gradients and radial electric fields present. Density gradients must be present when a plasma is confined. A typical variation of ion density with radius is shown in figure 3a. The fact that the ion density profile does not exactly fit a gaussian gives rise to non-uniform ion and electron angular diamagnetic velocities (figure 3b). Time independent radial electric fields can arise for several reasons. Since there is no accumulation of charge at the end plates, the thermal efflux of electrons from the plasma into the end plate sheath must be equal to the thermoelectric emission of electrons from the end plate. The flux of electrons from the plasma to the plate is given by:

$$J_F = 1/4\ n_o^e\ V_{TH}^e \qquad (2.15)$$

The electron flux emitted by the plate is given by the Richardson current:

$$J_E = AT^2 \exp\left[-\left(\frac{e\phi^w}{kT} + \frac{e\phi}{kT}\right)\right] \qquad (2.16)$$

where

ϕ^w = the work function for the end plate

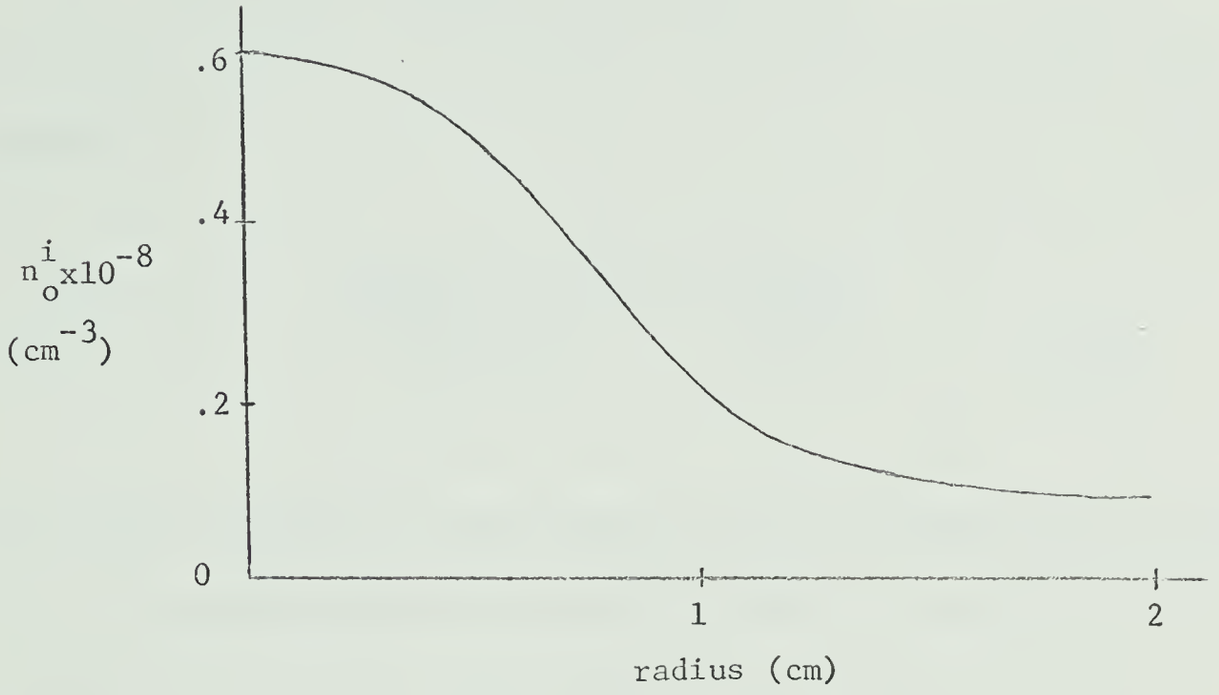

Figure 3a - Variation of ion density n_o^i with radius

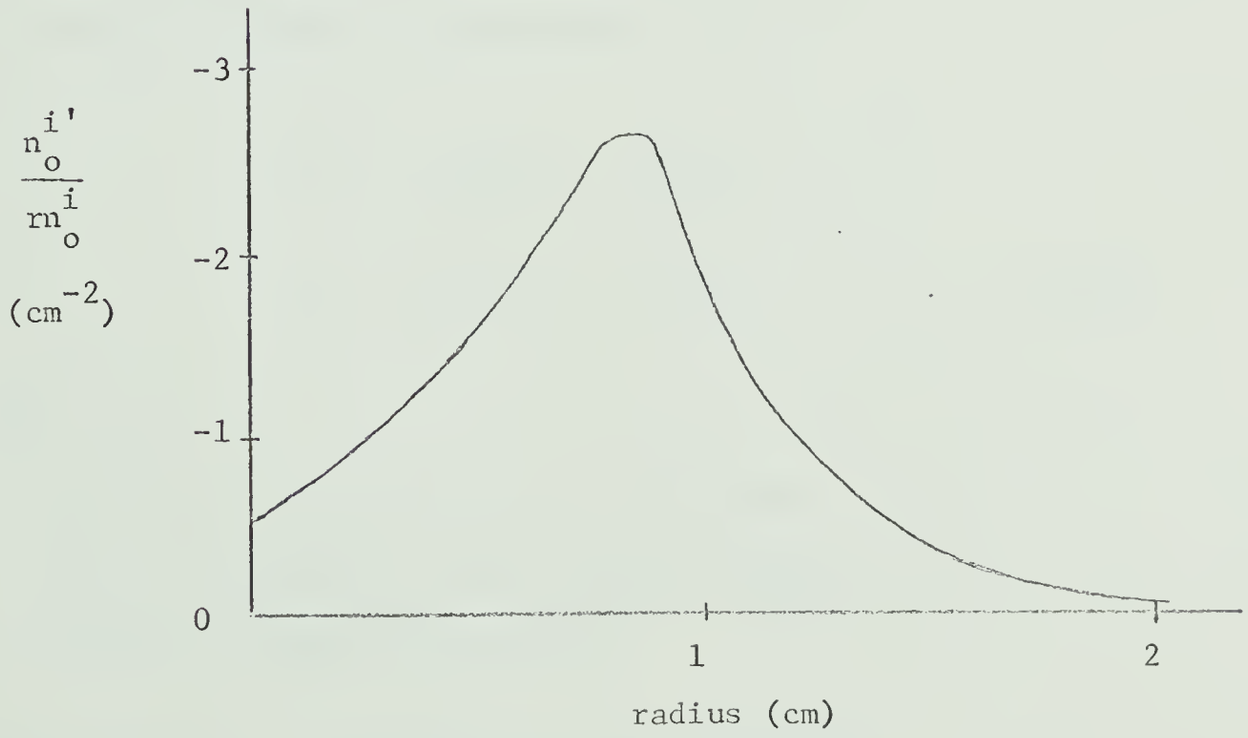

Figure 3b - Variation of $\frac{n_o^{i'}}{rn_o^i}$

ϕ = the potential of the plasma with respect to the end plate

$A = 1.0 \times 10^{29}$ electrons cm^{-2} sec^{-1} $^{o}K^{-2}$

By equating J_E with J_F, solving for ϕ and taking its gradient, one obtains[3]:

$$\vec{E} = -\nabla\phi = \frac{-kT}{e}\left(\frac{\nabla n_o^e}{n_o^e}\right) + \left(\phi^w - \phi + \frac{3kT}{2e}\right)\frac{\nabla T}{T} \qquad (2.17)$$

Thus density gradients in the plasma as well as temperature gradients in the end plates give rise to electric fields. Since the gradients are predominantly radial, the electric field will be radial. The diffusion and mobility of the ions and electrons can give rise to particle losses which result in electric fields. The electron and ion particle currents are given by:

$$\Gamma_e = -nU^e \cdot \vec{E} - D^e \cdot \nabla n$$

$$\Gamma_i = nU^i \cdot \vec{E} - D^i \cdot \nabla n \qquad (2.18)$$

where

$U^{e,i}$ = electron (ion) mobility tensor

$D^{e,i}$ = electron (ion) diffusion tensor

$n^e \simeq n^i$ = n (particle density)

By putting $\Gamma_e = \Gamma_i$ (steady state) one obtains:

$$\vec{E} = -\left[(U^e + U^i)^{-1}\right]\left[D^e - D^i\right]\cdot\frac{\nabla n}{n} \qquad (2.19)$$

Since electrons diffuse more rapidly than ions, an electric field will develop (equation 2.19) which will slow down the electrons, accelerate the ions and thus allow the two particle currents to become equal. Also, radial electric fields are often imposed externally on the plasma for purposes of investigation.[11] The end plate is split into two concentric parts separated by a small gap. By applying a voltage between these two sections, an adjustable radial electric field can be obtained. A typical variation of voltage with radius is given in figure 4a with the resulting angular electric drift velocity profile (figure 4b).

In the type of "Q-machine" just described one observes localized oscillations[3] near the region of maximum density gradient. These oscillations propagate with an azimuthal velocity of the same order of magnitude as the electron diamagnetic drift velocity. A standing wave exists in the radial direction (usually a zero'th radial mode) and in the axial direction (parallel wave length is approximately twice the machine length). The radial electric fields show a stabilizing influence when the electric rotation opposes the electron diamagnetic rotation[12].

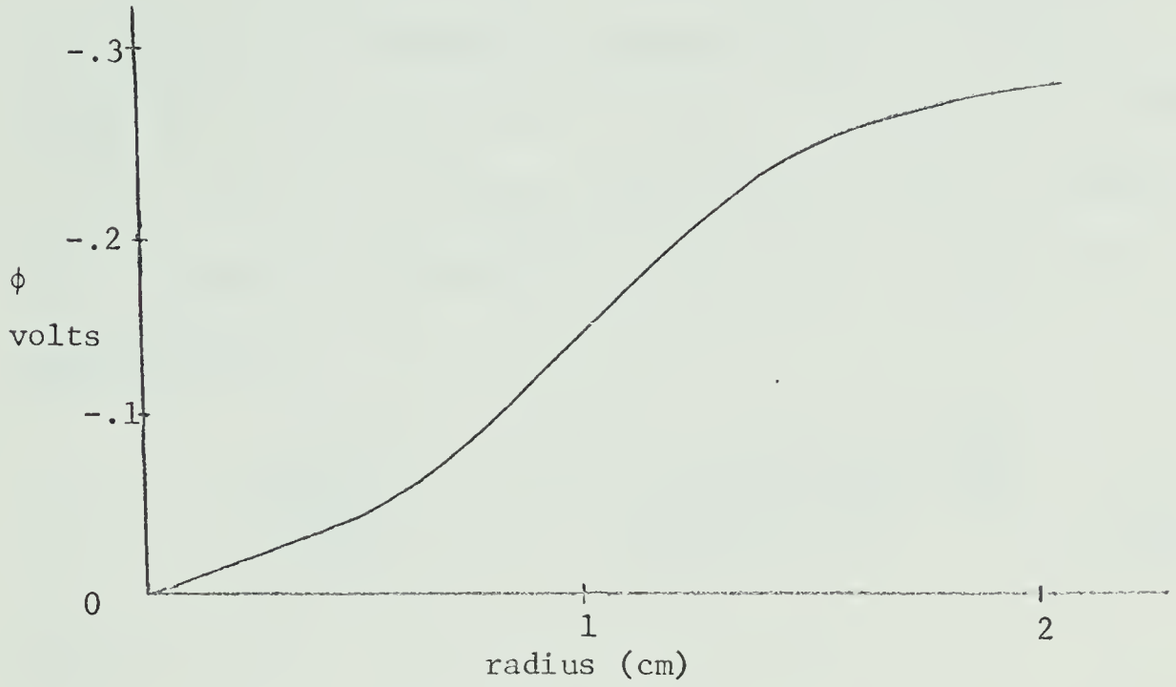

Figure 4a - Variation of voltage with radius

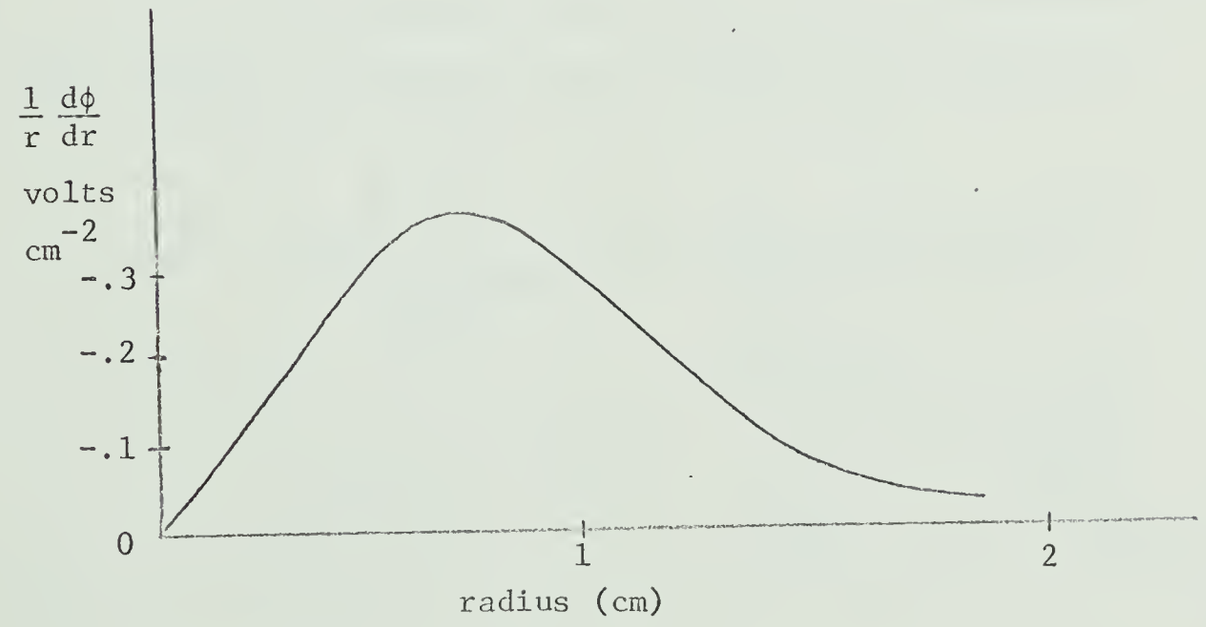

Figure 4b - Variation of $\frac{1}{r}\frac{d\phi}{dr}$ with radius

2.3 Theoretical Model

Any theoretical efforts to explain the properties of the drift mode must be modeled to the experimental situation described in the above section. This is accomplished by choosing suitable functions to represent the profiles shown in figures 3 and 4 (Capjack and Stringer[4]). The profile of figure 3b is represented as:

$$\left(\frac{1}{r}\frac{n_o^{i'}}{n_o^{i}}\right) = \alpha = \frac{-\left(1 + b\exp\left[-(r-r_M)^2/L_N^2\right]\right)}{L_N\, r_M\,(1+b)} \qquad (2.20)$$

where:

L_n = the density scale length

r_M = the radius at which α is maximum

b = the parameter representing the non-uniformity in α

The resulting ion density profile (figure 3a) is given by:

$$n_o^i = n_o \exp\left[\frac{-1}{L_N r_M(1+b)}\left\{\frac{r^2}{2} + bL_N\left[\frac{L_N}{2}\left(\exp\left[-(r_M/L_N)^2\right] - \exp\left[-(r-r_M)^2/L_N^2\right]\right) + r_M\int_{-r_M/L_N}^{(r-r_M)/L_N}\exp(-z^2)\,dz\right]\right\}\right] \qquad (2.21)$$

Finally, the profile of figure 4b is represented as:

$$\left(\frac{1}{r}\frac{\partial\phi}{\partial r}\right) = \left[10^8 \text{ Max}\left|\frac{1}{r}\frac{\partial\phi}{\partial r}\right| \text{volts/cm}^2 \text{ sgn}\left(\frac{1}{r}\frac{\partial\phi}{\partial r}\right) \text{sech}^2\left(\frac{r-r_M}{L_E}\right)\right] \quad (2.22)$$

where L_E = the electric scale length

It will be assumed that α and $(1/r\ \partial\phi/\partial r)$ are maximum at the same radius r_M. The electron diamagnetic frequency (W_{EN}), ion diamagnetic frequency $(W_\wedge)$, electric drift frequency (W_E) and the electron density (n_o^e) can all be determined from equations (2.20), (2.21) and (2.22). These are given as follows:

$$W_E = \frac{1}{B}\left(\frac{1}{r}\frac{\partial\phi}{\partial r}\right) = C_E \text{sech}^2\left(\frac{r-r_M}{L_E}\right) \quad (2.23)$$

$$W_\wedge = \frac{kT}{eB}\alpha = \frac{-C_{NE}(1 + b\exp\left[-(r-r_M)^2/L_N^2\right])}{(1+b)} \quad (2.24)$$

$$n_o^e = n_o^i\left[1 + (C_A/C)^2(2W_E + rW_E')/\Omega_i\right] \quad \text{(See A.4)} \quad (2.25)$$

$$W_{EN} = -W_\wedge - \left(\frac{kT}{eBr}\right)\left(\frac{C_A}{C}\right)^2\left[\frac{(2W_E + W_E'\chi-\alpha r) + (3W_E' + W_E''r)}{\Omega_i + (C_A/C)^2(2W_E + W_E'r)}\right] \quad (2.26)$$

where

C_E = Max(W_E)

C_{NE} = Max($W_{\wedge}$)

C_A = Alfvén velocity (Appendix A, equation A.4)

All the properties of the unperturbed plasma are assumed to be adequately described by equations (2.20 - 2.26). Table 1 gives the typical numerical values for the important plasma parameters found in "Q-machines". All subsequent approximations made are based on these values.

Table 1 - Plasma Parameters

n_o^e	.....electron density.....	$10^8/cm^3$
n_o^i	.....ion density.....	$10^8/cm^3$
a_i	.....ion Larmor radius.....	$5x10^{-2}$ cm
a_e	.....electron Larmor radius.....	$4x10^{-4}$ cm
T	.....electron or ion temperature.....	2000 ^oK
B	.....magnetic field (uniform).....	3000 Gauss
C_{NE}	.....peak diamagnetic rotation.....	$2x10^4$/sec
L_N	.....density scale length.....	$4x10^{-1}$cm
b	.....non-uniform rotation parameter.....	10
r_M	.....radius at peak rotation.....	$8x10^{-1}$cm
Ω_e	.....electron cylotron frequency.....	$5x10^{10}$/sec
Ω_i	.....ion cyclotron frequency.....	$4x10^6$/sec
$K_{\shortparallel}$	.....parallel wave number.....	$3x10^{-2}$/cm
V_{TH}^i	.....ion thermal velocity.....	$2x10^5$cm/sec
V_{TH}^e	.....electron thermal velocity.....	$2x10^7$cm/sec
r_p	.....plasma radius.....	2.5 cm
C_E	.....peak electric rotation.....	$\sim C_{NE}$
L_E	.....electric scale length.....	$\sim L_N$
M_e	.....electron mass.....	$9.1x10^{-28}$gm
M_i	.....ion mass (Lithium plasma).....	$11.7x10^{-24}$gm

CHAPTER III

ANALYSIS OF THE DRIFT MODE

3.1 Differential Equation

The differential equation describing the drift instability in the presence of non-uniform radial electric fields is derived in Appendix A for the variable ψ, which is the perturbed guiding centre displacement. The equation is:

$$\frac{1}{r}\frac{d}{dr}\left(S_o \frac{d\psi}{dr}\right) + \psi\left[\frac{(1-m^2)S_o}{r^3} + rW^2 n_o^{i\,\prime} - (C_A/C)^2 K_{\shortparallel}^2 n_o^i W_o^2 r^2\right]$$

$$- \psi\left[\frac{2r^2 W_o}{a_i^2}\left(n_o^e(W_o - mW_{EN})\, Z(W_o/K_{\shortparallel}V_{TH}^e) + n_o^i(W_o - mW_{\wedge})\, Z(W_o/K_{\shortparallel}V_{TH}^i)\right)\right] = 0 \qquad \text{(A.1)}$$

By making the substitution $\psi = S_o^{-\frac{1}{2}} y$ in the above equation, one obtains:

$$y'' - \frac{1}{a_i^2} Q(W,r) y = 0 \qquad (3.1)$$

where:

$$y(r) = \psi S_o^{-\frac{1}{2}} = \left(\frac{\phi_1}{W_o r}\right)\left[W_o r^3 n_o^i (W_o - mW_{\wedge} + W_o(C_A/C)^2)\right]^{-\frac{1}{2}}$$

$$Q(W,r) = \frac{2(W_o - mW_{EN})Z(W_o/K_{\shortparallel}V_{TH}^e) + 2(W_o - mW_{\wedge})Z(W_o/K_{\shortparallel}V_{TH}^i)}{W_o(1+(C_A/C)^2 - mW_{\wedge}/W_o)} + a_i^2 F_L(W,r)$$

$$F_L(W,r) = \frac{m^2-1}{r^2} + \frac{(C_A/C)^2 K_n^2 - (W/W_o)^2 \alpha}{(1+(C_A/C)^2 - mW_\wedge/W_o)} + \frac{1}{2}\left(\frac{S_o'}{S_o}\right)' + \frac{1}{4}\left(\frac{S_o'}{S_o}\right)^2$$

One can note that $a_i^2 F_L$ is of the order $(a_i/L)^2$ times that of the first or dominant term where L is a characteristic length (density or electric field scale length) in the plasma. The term $a_i^2 F_L$ is thus considered as a correction term associated with finite Larmor radius effects. The remainder of this chapter will deal with the solution of (3.1) for the real parts (W_R) and imaginary parts (W_I) of the complex frequency W.

3.2 WKB Solution, Local Approximation

It is assumed that Q has only two turning points z_1 and z_2 where $Q(z_1) = Q(z_2) = 0$. In order that a bounded solution exists, with the solution far from the turning points "joining smoothly" with the solution in the region of the turning points, the following quantization condition must hold in the complex plane:[5]

$$\frac{1}{a_i}\int_{z_1}^{z_2} \sqrt{-Q}\, dz = (n + \tfrac{1}{2})\pi \quad (n \text{ is an integer}) \qquad (3.2)$$

If the solutions $y(W,z)$ are to be analytically continued to the real "r" axis such that $y(W,r) \to 0$ as $r \to \infty$, the branch cuts from z_1 and z_2 must join at $z = \infty$ and the Anti-Stokes lines must cross the real axis (figure 5). The latter condition will always hold since Q is almost real with almost real turning points.

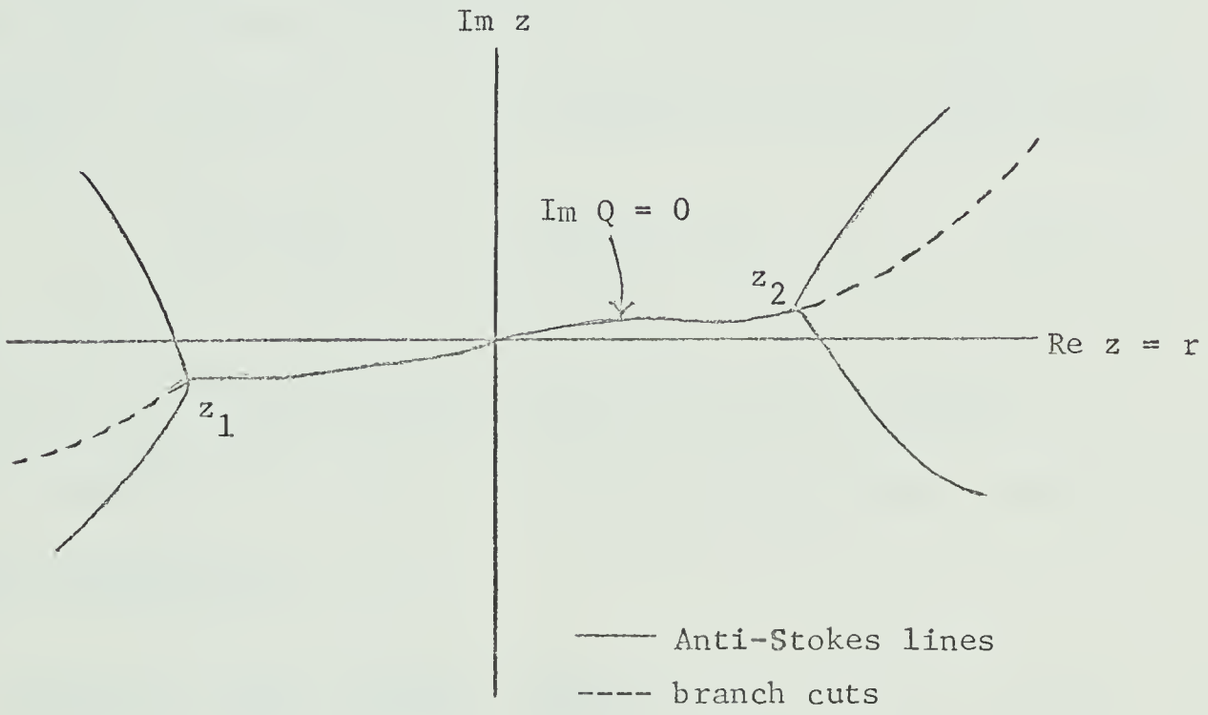

Figure 5 - Branch cuts and Anti-Stokes lines characteristic of a valid WKB solution.[5]

One now assumes that highly localized modes exist, implying that the turning points will be close together. Thus if Q is expanded in a Taylor series about the point z_o where $Q'(z_o) = 0$,

keeping terms to order $(z-z_o)^2$ only will result in a reasonable approximation for Q in the region between the turning points. If the expansion for Q is substituted in equation (3.2) the result is:

$$Q(z_o) = \frac{3(n + \frac{1}{2})\pi}{8} (-Q''a_i^2)^{\frac{1}{2}} \qquad (3.3)$$

The local approximation (Krall[1]) involves setting the right hand side of equation (3.3) equal to zero on the assumption that $(-Q''a_i^2)^{\frac{1}{2}} \sim O(a_i/L_N)^2 << 1$. The dispersion relation then becomes:

$$Q(z_o,W) = 0 \quad , \quad Q'(z_o,W) = 0 \qquad (3.4)$$

The function $Q(z_o,W)$ can be written as $f(z_o,W) + ig(z_o,W)$. If the assumptions that $|g| << |f|$ and $W_I << W_R$ are used, equation (3.4) can be written as:

$$Q(z_o,W) \simeq f(W_R) + ig(W_R) + i\frac{\partial f}{\partial W} W_I = 0 \qquad (3.5)$$

The dispersion relation then becomes:

$$f(W_R) = 0 \Big|_{z=z_o}$$

$$W_I = \frac{-g(W_R)}{\frac{\partial f}{\partial W}_{W=W_R}} \Bigg|_{z=z_o} \qquad (3.6)$$

Based on the physical arguments of chapter two, equation (3.1) will only be considered in the limits $V_{TH}^{i} << W_o/K_{\parallel} << V_{TH}^{e}$. The Z functions can then be written as:[13]

$$Z(W_o/K_{\parallel}V_{TH}^{e}) \simeq 1 + i\sqrt{\pi}W_o/K_{\parallel}V_{TH}^{e} \qquad (W_o/K_{\parallel}V_{TH}^{e}) << 1$$

$$Z(W_o/K_{\parallel}V_{TH}^{i}) \simeq -\tfrac{1}{2}(V_{TH}^{i}K_{\parallel}/W_o)^2 \qquad (W_o/K_{\parallel}V_{TH}^{i}) >> 1$$

Equation (3.6) is now used with:

$$f = \frac{2(W_o - mW_{EN}) - (V_{TH}^{i}K_{\parallel}/W_o)^2(W_o + mW_{EN}) + a_i^2 F_L W_o\left[1+(C_A/C)^2 - mW_{\wedge}/W_o\right]}{W_o\left[1+(C_A/C)^2 - mW_{\wedge}/W_o\right]}$$

$$g = \frac{2\sqrt{\pi}(W_o/K_{\parallel}V_{TH}^{e})(W_o - mW_{EN})}{W_o\left[1+(C_A/C)^2 - mW_{\wedge}/W_o\right]}$$

$$z_o = r_M$$

By keeping terms to first order in a_i^2 and $(V_{TH}^{i}K_{\parallel}/W_o)^2$ and assuming quasi-neutrality, one obtains the following expressions for the frequency and growth rate of the drift wave:

$$W_R^o = mW_{EN}\left[1 - a_i^2 F_L^* + (V_{TH}^i K_{\shortparallel}/W_R^o)^2\right]\Big|_{r=r_M}$$

$$W_I = (\sqrt{\pi} W_R^o/K_{\shortparallel}V_{TH}^e)(mW_{EN}-W_R^o) \simeq \frac{\sqrt{\pi}(mW_{EN})^2}{K_{\shortparallel}V_{TH}^e}\left[a_i^2 F_L^* - (V_{TH}^i K_{\shortparallel}/W_R^o)^2\right]\Big|_{r=r_M} \tag{3.7}$$

where

$$W_R^o = W - mW_E\Big|_{r=r_M} = W_R - mC_E$$

$$F_L^* = \left(\frac{m^2-\frac{1}{4}}{r^2}\right)(1+\tfrac{1}{2}(C_A/C)^2) + \frac{1}{4}\frac{W_{EN}''}{W_{EN}} - \frac{W_E''}{W_{EN}}\left(\frac{3+2(C_A/C)^2}{4}\right)$$

$$-\left(\frac{n_o^i}{2n_o^i r}\right)\left[\left(\frac{1+W_E}{W_{EN}}\right)^2 - 4\right] + \left(\frac{n_o^i}{2n_o^i}\right)^2\left(\frac{1+(C_A/C)^2}{1+\frac{1}{2}(C_A/C)^2}\right)$$

The result for the growth rate W_I is basically the same as that obtained in chapter two (equation 2.14) except the wave frequency W_R is replaced by W_R^o, the wave frequency in a reference frame rotating at the peak electric angular frequency C_E.

The effect of the radial electric field is to "doppler-shift" the wave frequency W_R. The finite Larmor radius effects, represented by the term $a_i^2 F_L^*$ give rise to a positive growth rate. Ion Landau damping is seen to have a stabilizing influence through the term $(V_{TH}^i K_{\parallel}/W_R^o)^2$. Since the dominant term $(m^2-\frac{1}{4})/r^2$ in F_L^* is magnified as $(C_A/C)^2$ increases, a lower density plasma should exhibit a higher growth rate. It will be seen in the next section that the local approximation cannot adequately describe the effects of a non-uniformity in the electric and diamagnetic rotations. This is because $(Q''a_i^2)^{\frac{1}{2}}$ turns out to be of the order (a_i/L_N) rather than $(a_i/L_N)^2$ when non-uniform effects become important. The local approximation then becomes invalid.

3.3 Weber-Hermite Approximation

Equation (3.1) will be approximated by a Weber-Hermite equation.[14] It will be shown that because of non-uniform rotations, the finite larmor radius affects the growth rate to order (a_i/L_N) rather than $(a_i/L_N)^2$ as in the local approximation.

In the region $V_{TH}^i << W_o/K_{\parallel} << V_{TH}^e$, $Q(W,r)$ can be written as:

$$Q(W,r) = \frac{2(W_o - mW_{EN})(1 + i\sqrt{\pi}W_o/K_{\parallel}V_{TH}^e)}{W_o(1 + (C_A/C)^2 + mW_{EN}/W_o)} + a_i^2 F_L(W,r) \qquad (3.8)$$

where the ion term has been ignored since it only contributes a very small stabilizing influence in the region of interest. Q is expanded about the values $r=r_M$ and $W=W^*=mC_{NE}+mC_E$ where terms of order $(r-r_M)^3$, $(W-W^*)^3$ and higher are ignored.

$$Q(W,r) = Q(W^*,r_M) + \frac{\partial Q}{\partial W}(W-W^*) + \frac{\partial^2 Q}{\partial W^2}\frac{(W-W^*)^2}{2} + \frac{\partial^2 Q}{\partial r^2}\frac{(r-r_M)^2}{2} \quad (3.9)$$

The assumptions made in equation (3.9) are:

i. The values of W_R^o to be obtained are close to mC_{NE}, the peak electron diamagnetic frequency. Thus the terms $(W_R^o-mC_{NE})^n\, Q^n(W)/n!$ can be ignored for $n > 3$. Also, the growth rate W_I is assumed to be much less than W_R^o.

ii. The modes are localized. Thus the magnitude of the eigenfunctions are appreciable only in the region $(r-r_M)/L_N << 1$ where the expansion in equation (3.9) will be valid.

iii. Q has only two turning points.

iv. Q is essentially an even function of $(r-r_M)$.

v. The term $a_i^2 F_L(W,r)$ is made constant at the value $a_i^2 F_L(W^*,r)$. Since this term is considered a small correction to Q, its variation within the region of localization can be ignored without greatly affecting the final results.

By evaluating the terms in equation (3.9) one obtains:

$$Q(W,r) \simeq (1 + i\sqrt{\pi m C_{NE}/K_{\prime\prime} V_{TH}^e})\left[\frac{(W-W^*)}{(mC_{NE})(1+\frac{1}{2}(C_A/C)^2)}\right] + a_i^2 F_L(W^*,r_M)$$

$$+\left[\frac{(1 + i\sqrt{\pi m C_{NE}/K_{\prime\prime} V_{TH}^e})}{(mC_{NE})^2(1+\frac{1}{2}(C_A/C)^2)}\right]\left[\frac{1}{2(1+\frac{1}{2}(C_A/C)^2)} - \frac{1}{(1+i\sqrt{\pi m C_{NE}/K_{\prime\prime} V_{TH}^e})}\right](W-W^*)^2$$

$$+\left[\frac{(1 + i\sqrt{\pi m C_{NE}/K_{\prime\prime} V_{TH}^e})}{(1+\frac{1}{2}(C_A/C)^2)}\right]\left[\frac{b}{1+b} + \frac{(C_E/C_{NE})}{(L_E/L_N)^2}\right]\left(\frac{r-r_M}{L_N}\right)^2 \qquad (3.10)$$

The differential equation (3.1) can now be written as:

$$y'' + \left[\lambda - A^2(r-r_M)^2\right]y = 0 \qquad (3.11)$$

where

$$\lambda = \frac{(1 + i\sqrt{\pi m C_{NE}/K_{\parallel} V_{TH}^{e}})\,(W^{*}-W)}{a_i^2\,(mC_{NE})\,(1+\frac{1}{2}(C_A/C^2)} \quad - \quad F_L(W^{*}, r_M)$$

$$+ \left[\frac{(1 + i\sqrt{\pi m C_{NE}/K_{\parallel} V_{TH}^{e}})}{(mC_{NE})^2(1+\frac{1}{2}(C_A/C)^2)}\right]\left[\frac{-1}{2(1+\frac{1}{2}(C_A/C)^2)} + \frac{1}{(1+i\sqrt{\pi m C_{NE}/K_{\parallel} V_{TH}^{e}})}\right]\frac{(W-W^{*})^2}{a_i^2}$$

$$A = \left[\frac{(1 + i\ \ mC_{NE}/K_{\parallel} V_{TH}^{e})}{(1+\frac{1}{2}(C_A/C)^2)}\ \left(\frac{b}{1+b} + \frac{(C_E/C_{NE})}{(L_E/L_N)^2}\right)\right]^{\frac{1}{2}}\left(\frac{1}{a_i L_N}\right)$$

Equation (3.11) is just the Weber-Hermite equation. In order that $y \to 0$ as $|r-r_M| \to \pm\infty$ (condition for localized modes) the following condition must be satisfied.

$$\lambda = (2n+1)A \qquad (3.12)$$

When the expressions for λ and A are substituted in equation (3.12) and terms of order $(mC_{NE}/K_{\parallel} V_{TH}^{e})^2$ are ignored, the following expressions for the "doppler-shifted" frequency (W_R^{o}) and the growth rate (W_I) are obtained:

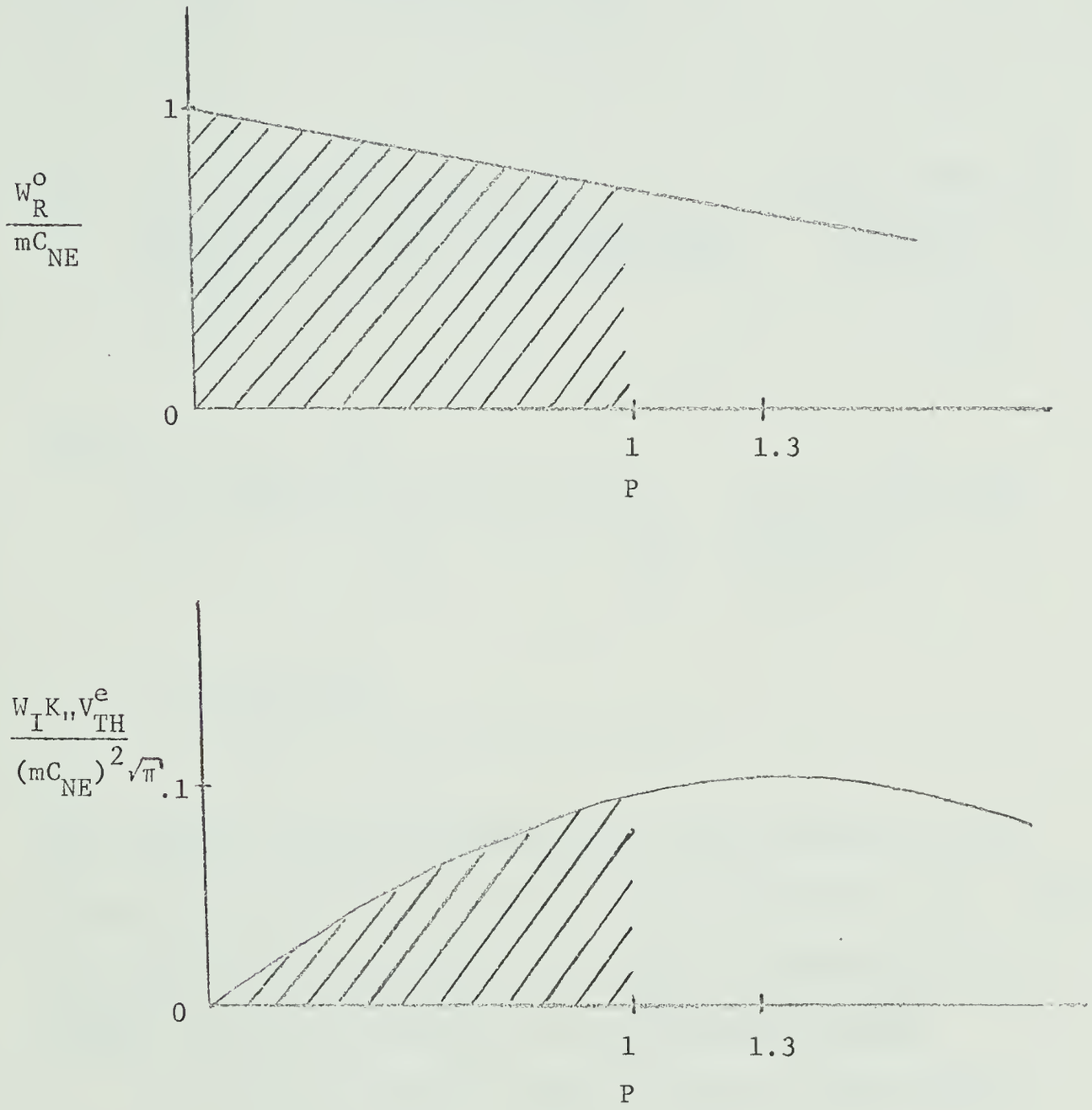

Figure 6 - Growth rate and frequency versus the important plasma parameters represented through the variable P. (See equation 3.13)

$$W_R^o = mC_{NE}\left[1 - \frac{\sqrt{1+P(1-1/2D)} - 1}{2(1-1/2D)}\right]$$

$$W_I = \left(\frac{\sqrt{\pi}}{K_{\shortparallel} V_{TH}^e}\right)\frac{(mC_{NE})^2}{2}\left[\frac{(3/2-1/4D)P}{2(1-1/2D)\sqrt{1+P(1-1/2D)}} - \frac{\sqrt{1+P(1-1/2D)} - 1)}{(1-1/2D)^2}\right] \qquad (3.13)$$

where

$$P = 4(2n+1)(a_i/L_N)\left[(1+\tfrac{1}{2}(C_A/C)^2)\left(\frac{b}{1+b} + \frac{(C_E/C_{NE})}{(L_E/L_N)}\right)\right]^{\frac{1}{2}} + 4a_i^2 F_L^*$$

$$D = (1+\tfrac{1}{2}(C_A/C)^2)$$

The variable P contains the important plasma parameters which determine the frequency and growth rate of the drift wave. Figure 6 shows W_R^o and W_I as functions of P. Only the shaded region of figure 6 will be of interest for the following reasons:

i. The approximations made in equation (3.10) become invalid as P becomes of the order unity.

ii. Experimentally, the modes of interest are for $W_R^o \simeq mC_{NE}$, which implies that $P \ll 1$.

In the limit that $P \ll 1$, the following expressions for the frequency, growth rate, eigenfunction and "potential well" Q pertaining to the

drift mode are obtained:

$$W_R^o = mC_{NE}\left\{1 - (2n+1)\ (a_i/L_N)\left[(1+\tfrac{1}{2}(C_A/C)^2)\left(\frac{b}{1+b} + \frac{(C_E/C_{NE})}{(L_E/L_N)^2}\right)\right]^{\frac{1}{2}} - a_i^2 F_L^*\right\} \tag{3.14}$$

$$W_I = \frac{\sqrt{\pi}(mC_{NE})^2}{2K_{\shortparallel}V_{TH}^e}\left\{(2n+1)(a_i/L_N)\left[(1+\tfrac{1}{2}(C_A/C)^2)\left(\frac{b}{1+b} + \frac{(C_E/C_{NE})}{(L_E/L_N)^2}\right)\right]^{\frac{1}{2}} + a_i^2 F_L^*\right\}$$

$$\simeq \frac{\sqrt{\pi}W_R^o}{K_{\shortparallel}V_{TH}^e}\ \frac{(mC_{NE} - W_R^o)}{2} \tag{3.15}$$

$$y_n(r) = H_n\left[\sqrt{2}A\ (r-r_M)\right]\ \exp\left[-A(r-r_M)^2/2\right] \tag{3.16}$$

where H_n are Hermite polynomials

$$Q(W,r) = \frac{-(1+i\sqrt{\pi}mC_{NE}/K_{\shortparallel}V_{TH}^e)}{(1+\tfrac{1}{2}(C_A/C)^2)^{\frac{1}{2}}}\left[(2n+1)\left(\frac{a_i}{L_N}\right)\left(\frac{b}{1+b} + \frac{(C_E/C_{NE})}{(L_E/L_N)^2}\right)^{\frac{1}{2}} + a_i^2 F_L - iW_I\right]$$

$$+\left[\frac{(1 + i\sqrt{\pi}mC_{NE}/K_{\shortparallel}V_{TH}^e)}{(1+\tfrac{1}{2}(C_A/C)^2}\right]\left(\frac{b}{1+b} + \frac{(C_E/C_{NE})}{(L_E/L_N)^2}\right)\left(\frac{r-r_M}{L_N}\right)^2 \tag{3.17}$$

The important feature in the above equations is that non-uniformities in the electric and diamagnetic rotation profiles, represented by the term $\sqrt{\frac{b}{1+b} + \frac{(C_E/C_{NE})}{(L_E/L_N)^2}}$, have a far greater affect on the growth rate of the wave than does the normal destabilizing term $a_i^2 F_L^*$ found in the local approximation. This is because the growth rate, which depends on terms of the order $(a_i/L_N)^2$ when non-uniformities are absent, now depends on terms of the order (a_i/L_N) (equation 3.15).

3.4 Numerical Solution

The numerical solution of equation (3.1) was obtained using the method of Appendix B. The numerical results given here illustrate the analytical results of equations (3.14 - 3.17) for the frequencies, growth rates, eigenfunctions and "potential wells" pertaining to the drift mode. The regions for which Q has four turning points are also investigated. Only the first radial mode will be of interest (n=0) since this is the one that is usually observed experimentally. All parameters are given as in Table 1 unless otherwise specified.

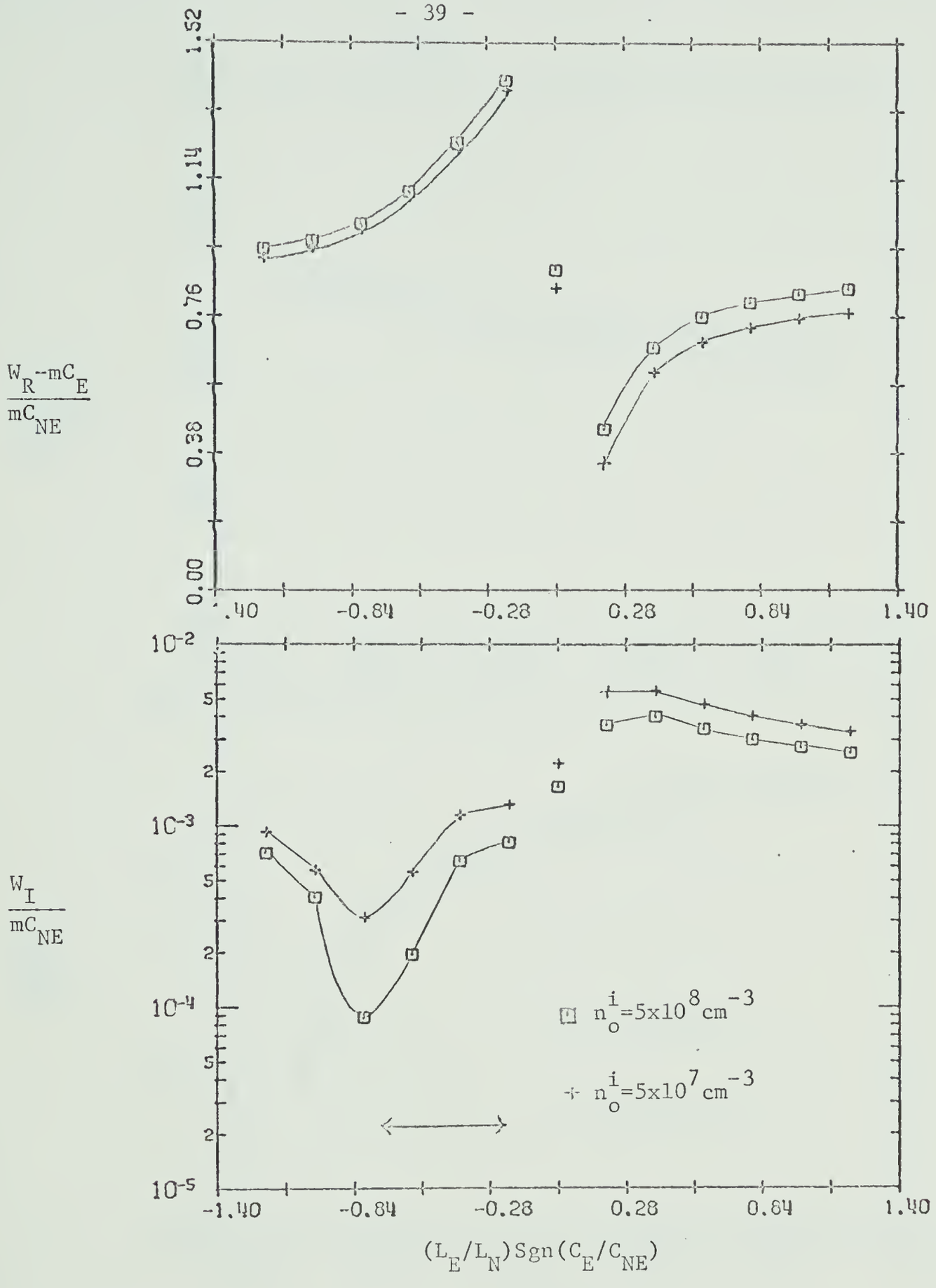

Figure 7 - The doppler-shifted frequency and the growth rate are shown as functions of (L_E/L_N) for peak ion densities of $5x10^7$ and $5x10^8$ cm^{-3}. (C_E/C_{NE}) takes on the values +.8, -.8 and 0. The azimuthal mode number m=1. $\longleftrightarrow$ depicts the region for which Q has four turning points.

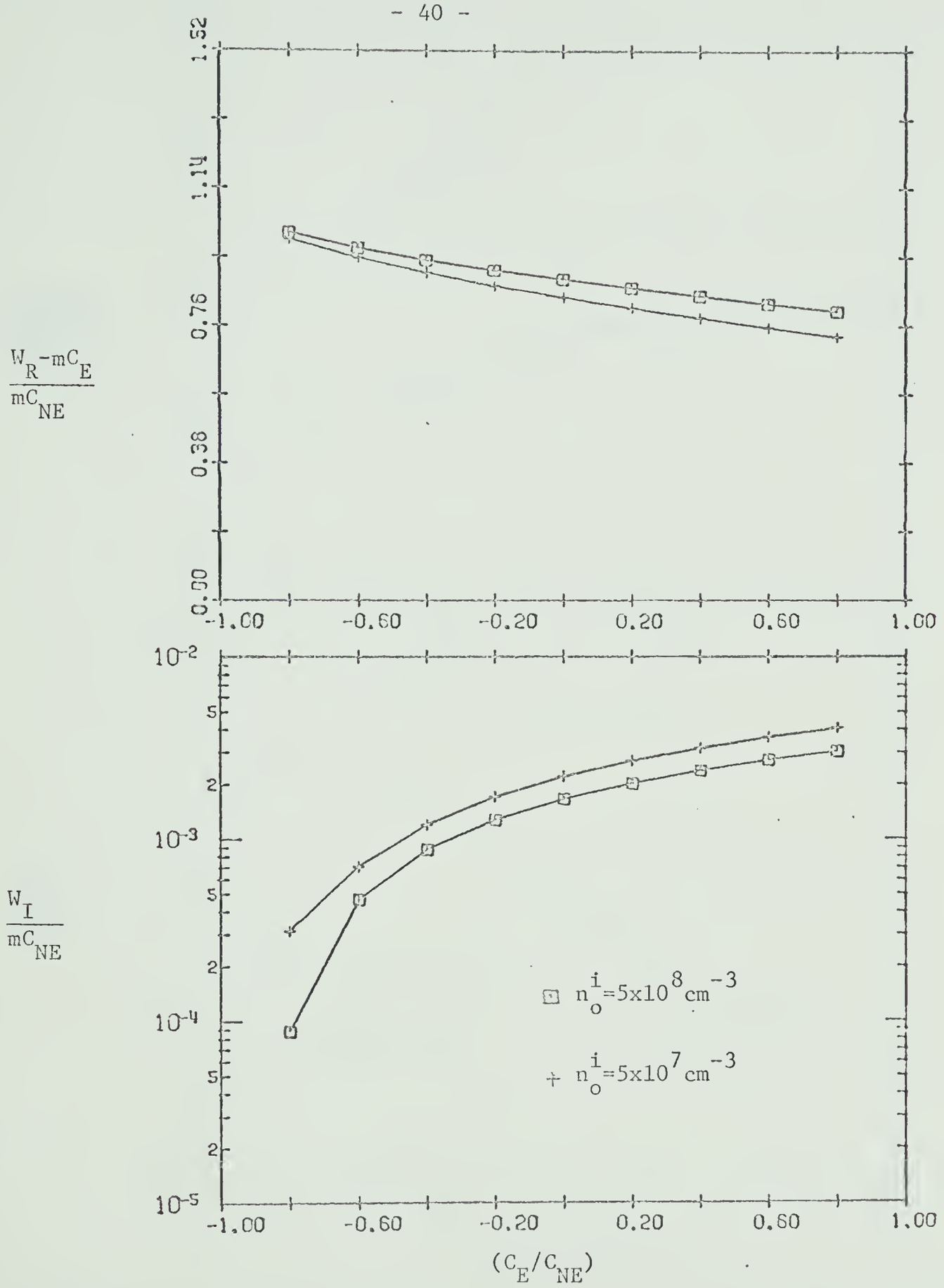

Figure 8 - The doppler-shifted frequency and the growth rate are shown as functions of (C_E/C_{NE}) for peak ion densities of $5x10^7$ and $5x10^8 cm^{-3}$. $(L_E/L_N) = .8$. The azimuthal mode number m=1.

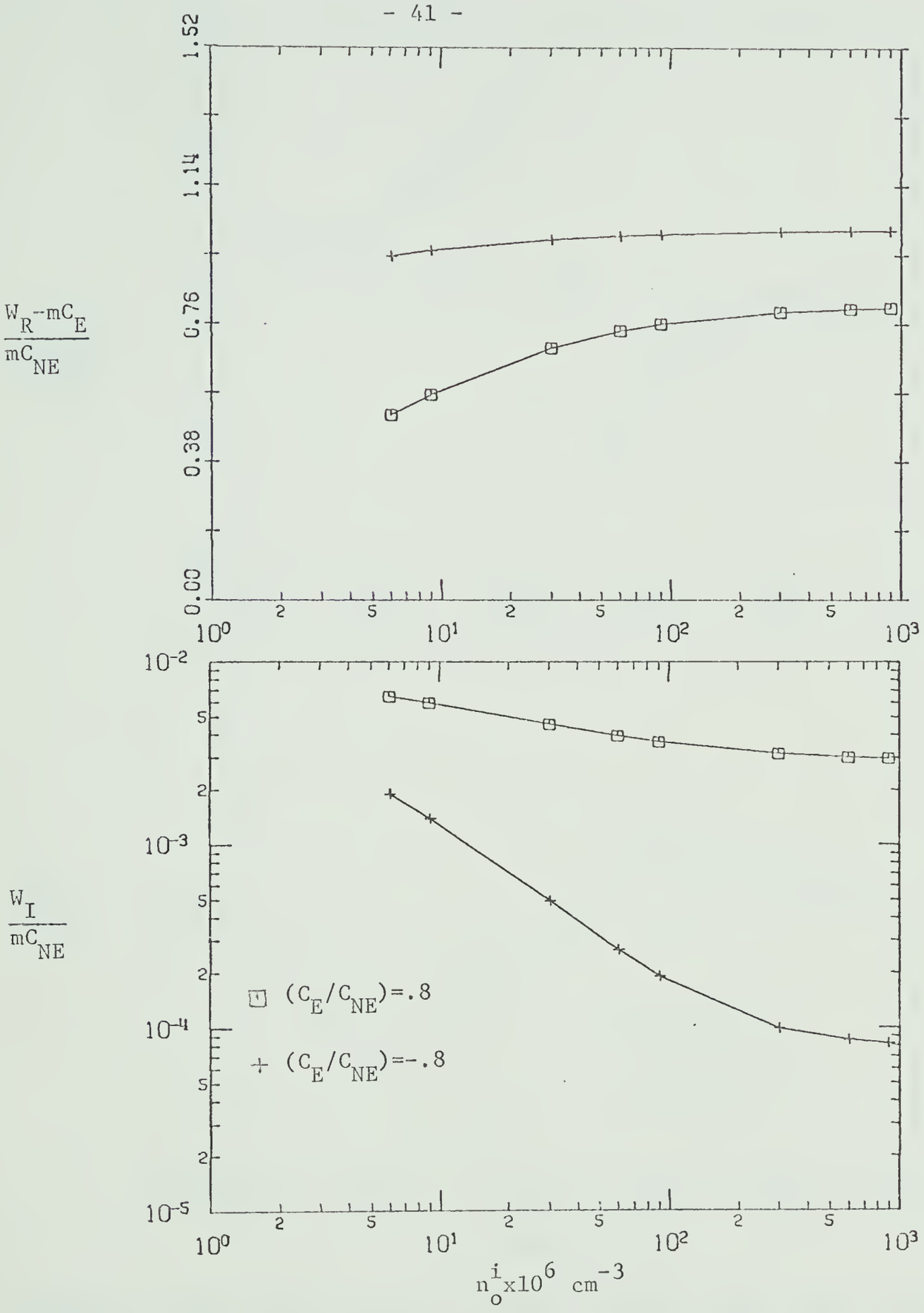

Figure 9 - The doppler-shifted frequency and growth rate are shown as functions of density for $(C_E/C_{NE}) = \pm.8$, $(L_E/L_N)=.8$. The azimuthal mode number m=1.

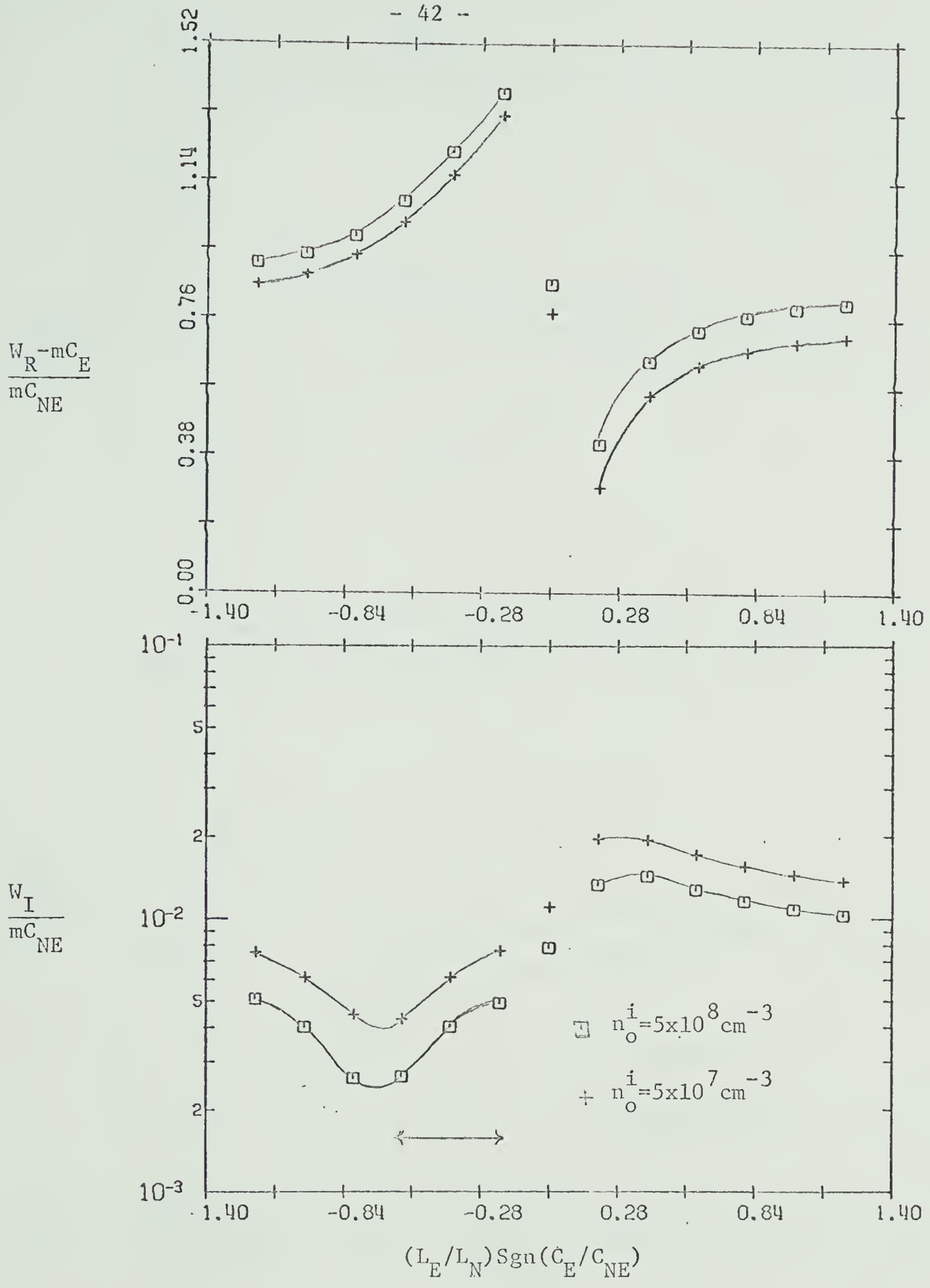

Figure 10 - The doppler-shifted frequency and the growth rate are shown as functions of (L_E/L_N) for peak ion densities of $5x10^7$ and $5x10^8$ cm^{-3}. (C_E/C_{NE}) takes on the values +.8, -.8 and 0. The azimuthal mode number m=3. ⟷ depicts the region for which Q has four turning points.

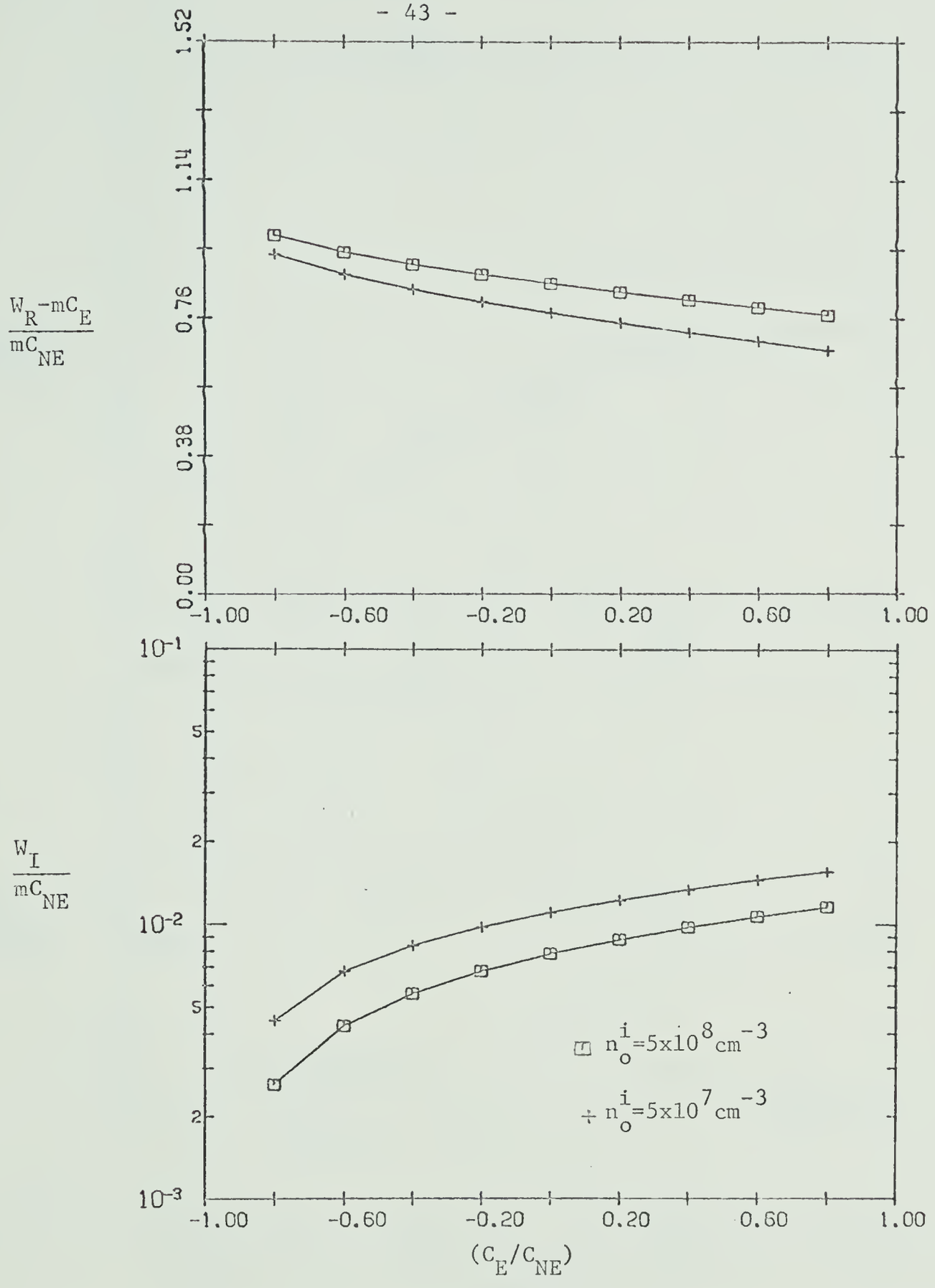

Figure 11 - The doppler-shifted frequency and the growth rate are shown as functions of (C_E/C_{NE}) for peak ion densities of 5×10^7 and $5 \times 10^8 cm^{-3}$. $(L_E/L_N) = .8$. The azimuthal mode number m=3.

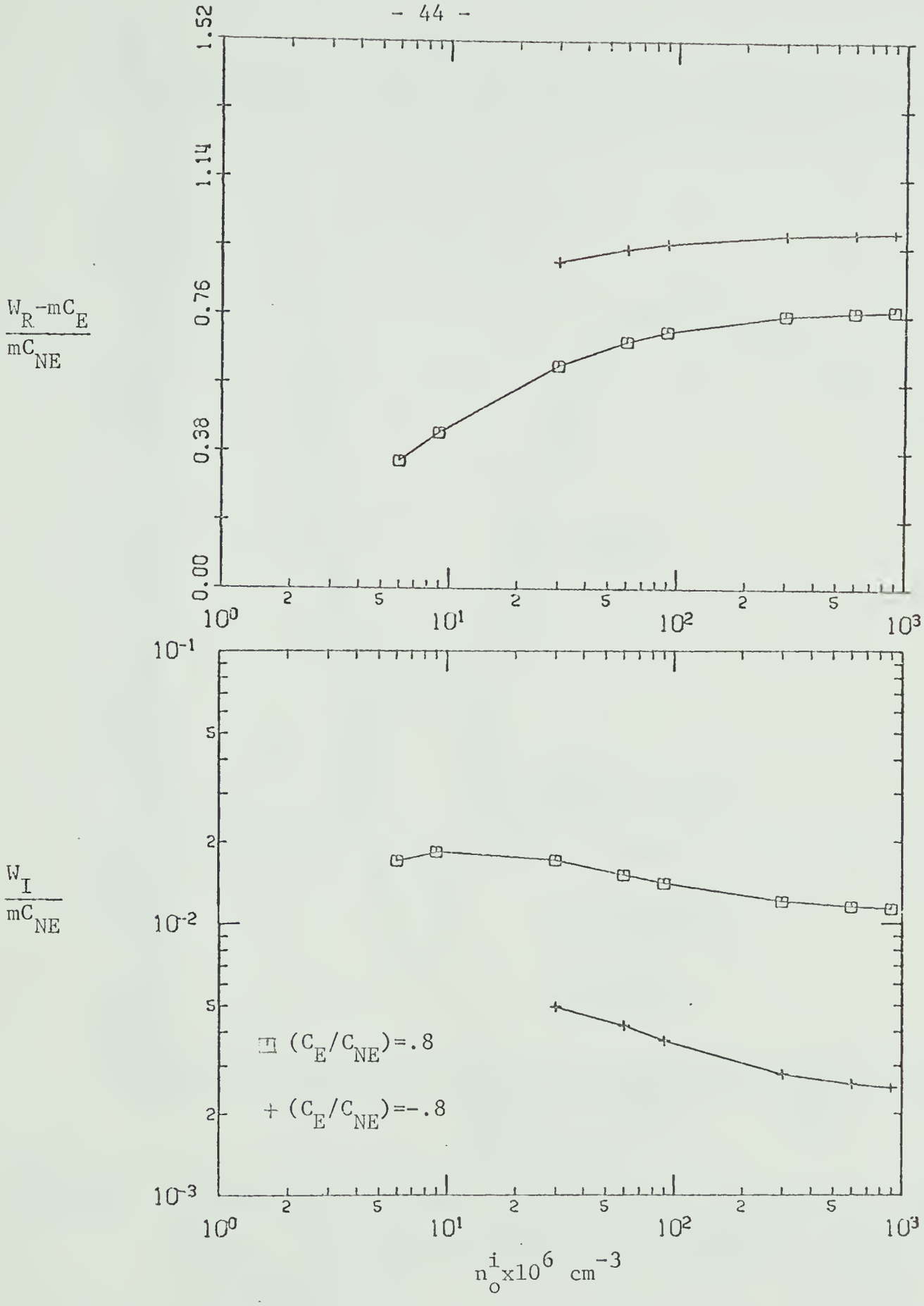

Figure 12 - The doppler-shifted frequency and growth rate are shown as functions of density for $(C_E/C_{NE}) = \pm.8$, $(L_E/L_N)=.8$. The azimuthal mode number m=3.

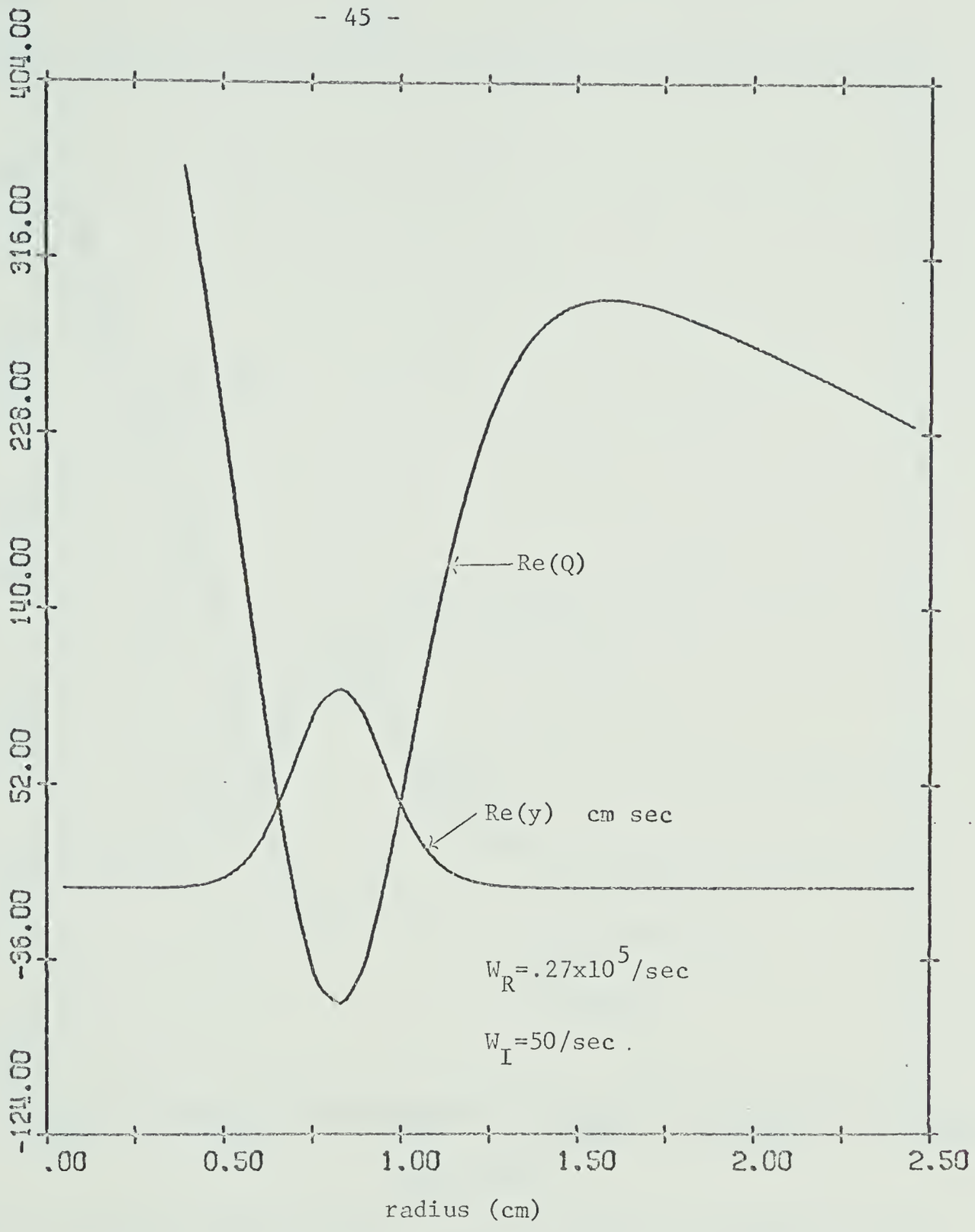

Figure 13 - The real parts of Q and $y_o(r)$ are shown as functions of the radius r. The peak ion density $n_o^i = 5\times10^8 cm^{-3}$. (C_E/C_{NE}) = .8, (L_E/L_N) = .8

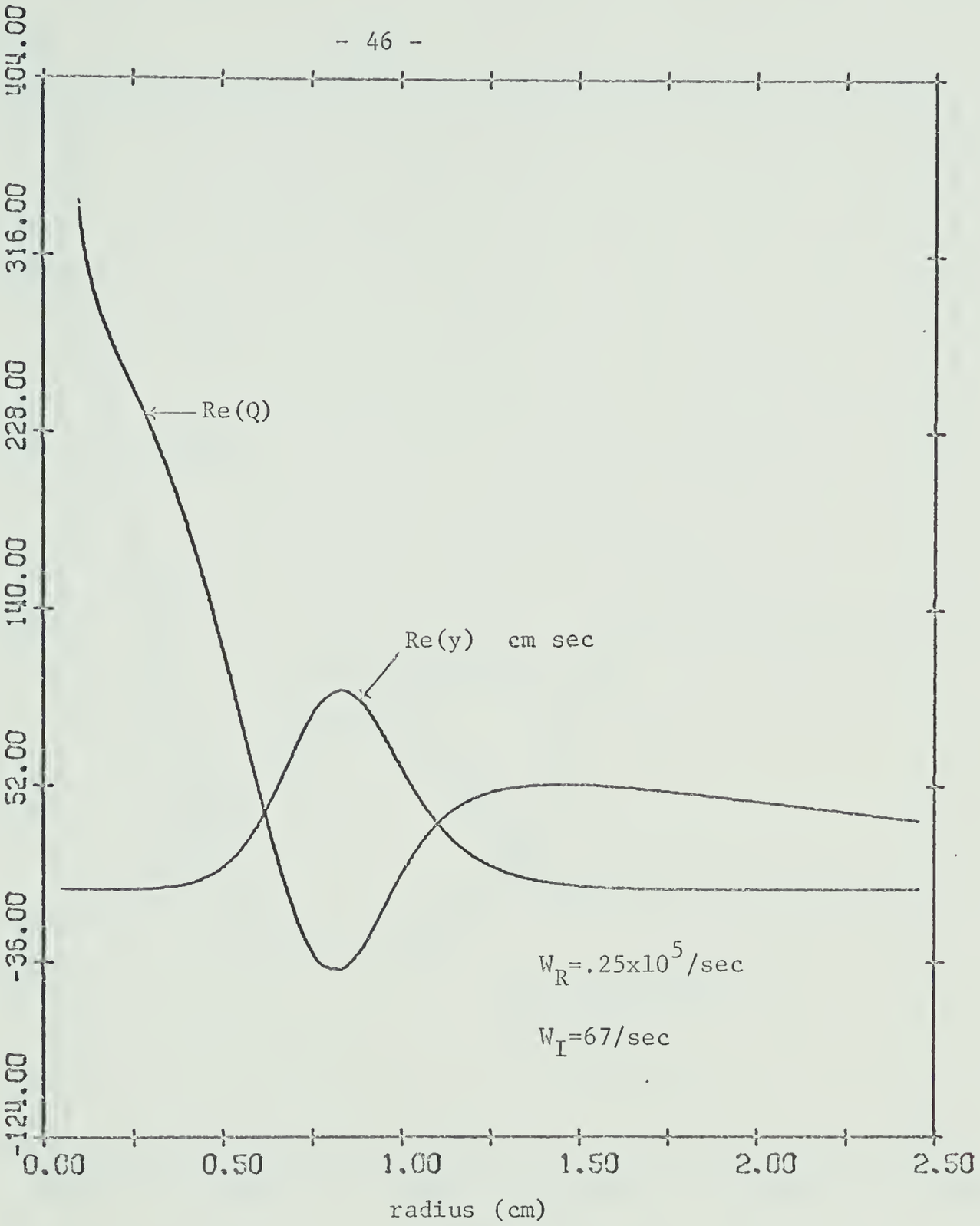

Figure 14 - The real parts of Q and $y_o(r)$ are shown as functions of the radius r. The peak ion density $n_o^i = 5\times10^7 cm^{-3}$. (C_E/C_{NE}) = .8, (L_E/L_N) = .8

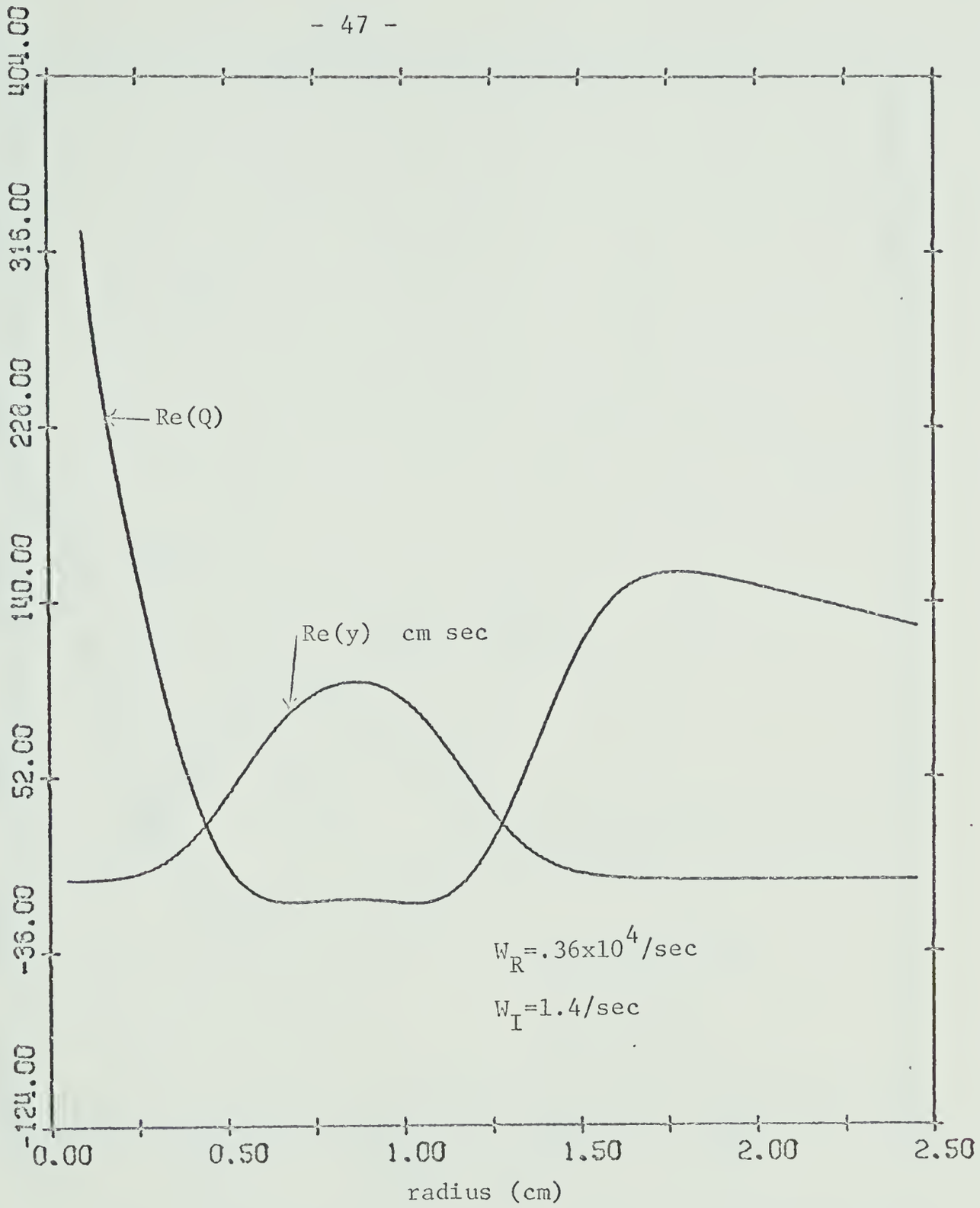

Figure 15 - The real parts of Q and $y_o(r)$ are shown as functions of the radius r. The peak ion density $n_o^i = 5\times10^8 cm^{-3}$. $(C_E/C_{NE}) = -.8$, $(L_E/L_N) = .8$

The above diagram depicts the eigenfunction and the "potential well" Q when the growth rate is minimized.

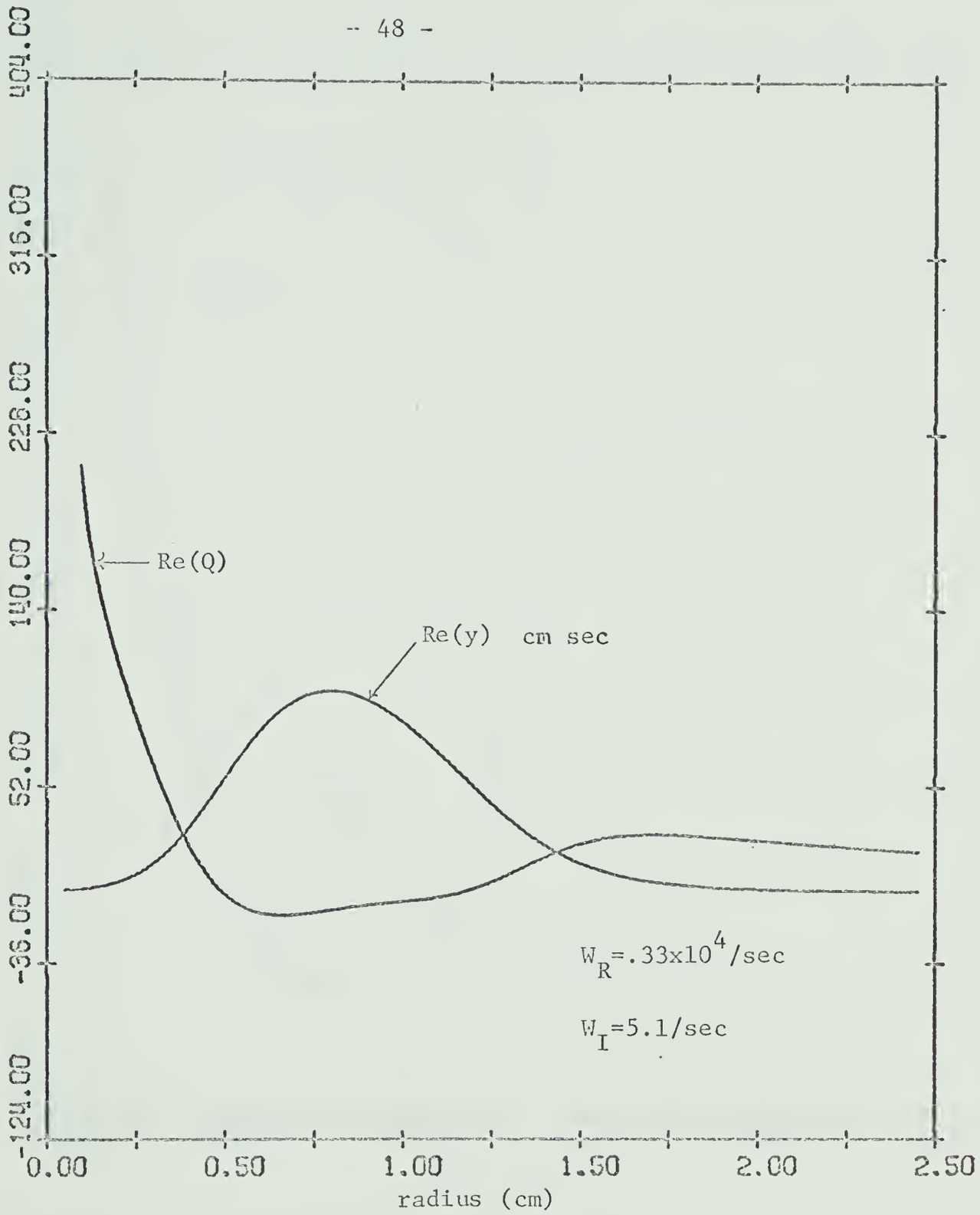

Figure 16 - The real parts of Q and $y_o(r)$ are shown as functions of the radius r. The peak ion density $n_o^i = 5\text{x}10^7 cm^{-3}$. (C_E/C_{NE}) = -.8, (L_E/L_N) = .8

The above diagram depicts the eigenfunction and the "potential well" Q when the growth rate is minimized. However, the plasma density is reduced from that of figure 15.

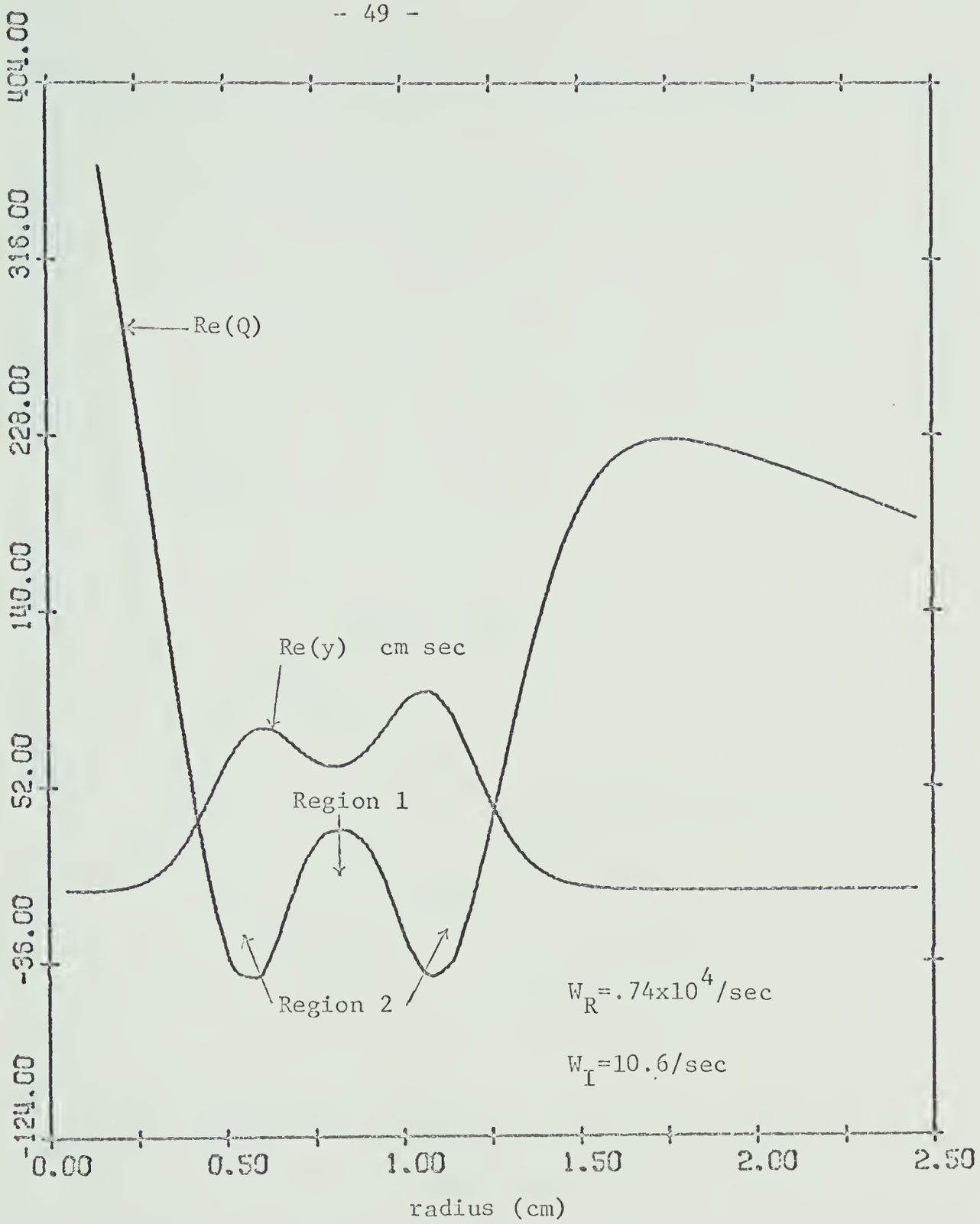

Figure 17 - The real parts of Q and $y_o(r)$ are shown as functions of the radius r. The peak ion density $n_o^i = 5 \times 10^8 cm^{-3}$. $(C_E/C_{NE}) = -.8$, $(L_E/L_N) = .4$. It can be noted that Q has four turning points.

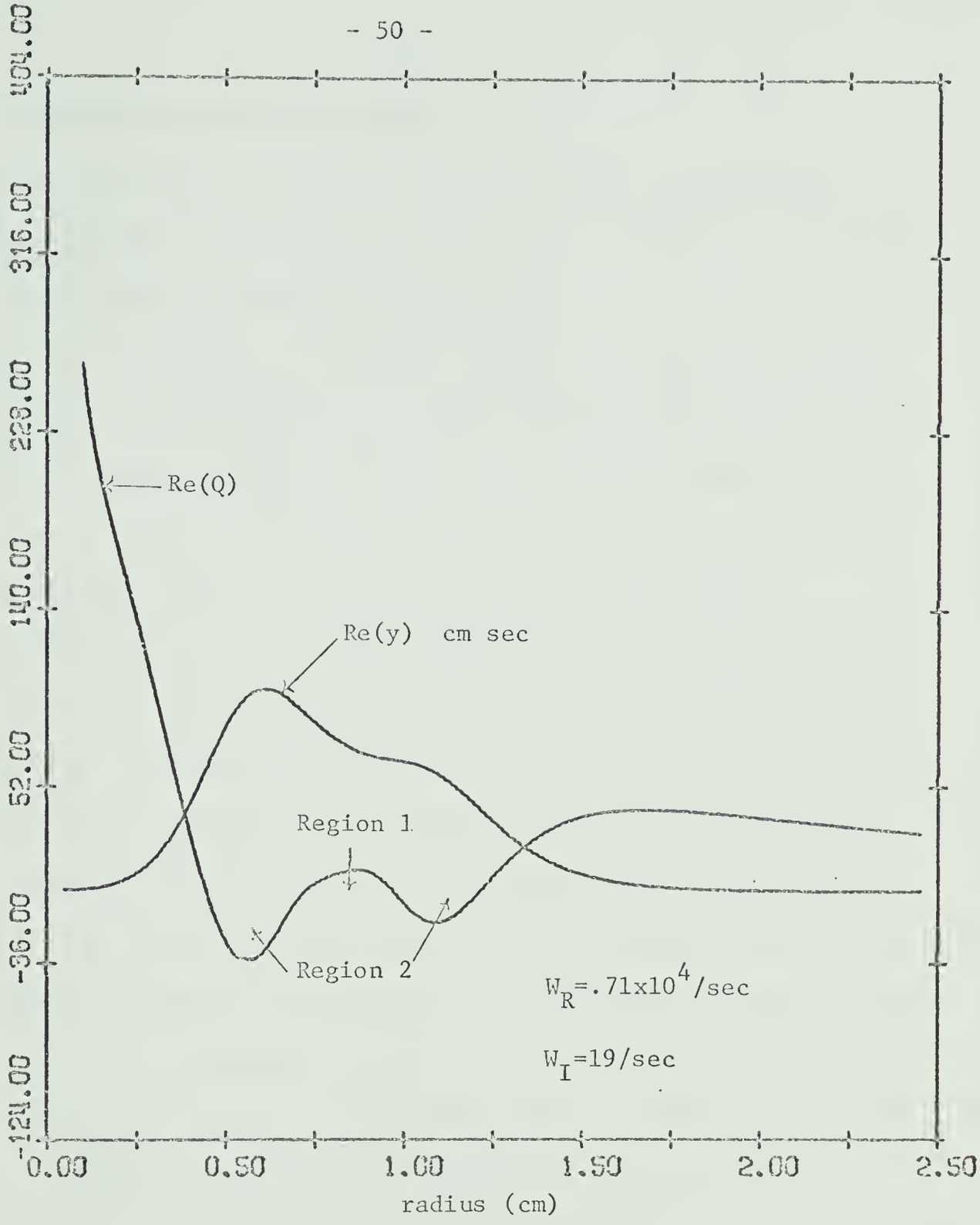

Figure 18 - The real parts of Q and $y_o(r)$ are shown as functions of the radius r. The peak ion density $n_o^i = 5x10^7 cm^{-3}$. (C_E/C_{NE}) = -.8, (L_E/L_N) = .4

The stabilizing region (region 1) has been reduced from that of figure 17 as a result of a decrease in density.

3.5 Interpretation and Discussion

From the previous sections it is seen that the growth rate depends strongly on the non-uniformity of the diamagnetic rotation and on the manner in which the electric rotation interacts with the diamagnetic rotation. The electric rotation has little effect on the growth rate when the electric scale length is much greater than the density scale length. When the electric scale length becomes less than or equal to the density scale length, the growth rate can be strongly affected by the electric rotation. This is physically reasonable since the velocity shear resulting from the non-uniform electric rotation can distort the distribution function giving rise to instability (section 2.1). The effects of this velocity shear become more pronounced when the electric rotation varies appreciably over a region of the order of the density scale length. When C_E is less than zero (electric rotation opposes the diamagnetic rotation), the electric rotation tends to cancel the non-uniformity in the diamagnetic rotation. The eigenfunction becomes delocalized and the growth rate drops (figure 15, equations 3.15 and 3.16). When C_E and L_E have values which best cancel the non-uniformities in the diamagnetic rotation, the growth rate is minimized and $W_R^o = mC_{NE}$ (figure 7).

When $\left[\frac{b}{1+b} + \frac{(C_E/C_{NE})}{(L_E/L_N)^2}\right] < 0$, the Weber-Hermite approximation becomes invalid since the "potential" function Q develops four turning

points. The numerical results show that as $\frac{(C_E/C_{NE})}{(L_E/L_N)^2}$ becomes increasingly negative, the growth rate again increases while the eigenfunction localizes over the negative portions of the "potential well" (figure 17). This behavior in the growth rate can be understood from the following argument. If equation (3.1) is multiplied by the complex conjugate of y and integrated from 0 to the edge of the cylinder r_p, one obtains:

$$\int_0^{r_p} \left|\frac{dy}{dr}\right|^2 dr + \int_0^{r_p} \frac{Q|y|^2}{a_i^2} dr = 0 \qquad (3.18)$$

$$\int_0^{r_p} \mathrm{Im}(Q)\,|y|^2\, dr = 0$$

By ignoring the small imaginary part of $a_i^2 F_L$ equation (3.18) yields:

$$W_I = \frac{\frac{\sqrt{\pi}}{2K_{\parallel}V_{TH}^e}\int_0^{r_p} \frac{(W_o - mW_{EN})(W_o)\ |y|^2}{W_o\left[1+(C_A/C)^2+mW_{EN}/W_o\right]}\, dr}{\int_0^{r_p} \frac{(2+(C_A/C)^2)(mW_{EN})\ |y|^2}{W_o^2\left[1+(C_A/C)^2+mW_{EN}/W_o\right]^2}\, dr} \qquad (3.19)$$

By letting only the essential quantities vary in the region where $|y(r)|$ is appreciable, equation (3.19) becomes:

$$W_I = \sqrt{\pi}\,\overline{(mW_{EN} - W_o)}\left(\frac{W_o}{K_{\parallel}V_{TH}^e}\right) \qquad (3.20)$$

where "$\overline{\qquad\qquad}$" denotes an averaging process with the eigenfunction acting as a probability distribution. Thus the growth rate is determined by what the wave "feels" over the whole region of the plasma. When Q has two turning points, $(mW_{EN}-W_o)$ is always positive over the region of wave localization (figure 13). When Q has four turning points, $(mW_{EN}-W_o)$ can become negative in regions where the wave amplitude is appreciable (region 1 of figure 17) thus contributing a stabilizing influence. However, the eigenfunction is then found to be strongly localized over the most unstable region (region 2 of figure 17). This is why a "potential well" with four turning points will not minimize the growth rate. The growth rate is found to be minimized when the "potential well" is as broad and shallow as possible. The analytical results (equations 3.15 and 3.16) suggest that this occurs when the electric rotation effectively cancels the non-uniformity in the diamagnetic rotation.

The effect of a decrease in density on the modes considered is to decrease the wave frequency and increase the growth rate. A decrease in density seems to have the most influence when the electric rotation opposes the diamagnetic rotation in such a manner as to give

a minimal growth rate. This is best observed in figure 7 and figure 9. However, decreasing the density even by a factor of ten does not change the manner in which the non-uniform rotations affect the growth rate. It would seem that terms involving $(C_A/C)^2$ can be ignored with little consequence to the qualitative results for densities in the range $5x10^7$ to $5x10^8$ particles/cm^3.

CHAPTER IV

CONCLUSION

The collisionless drift wave, with a component of the propagation vector parallel to the magnetic field, has been examined in a cylindrical plasma for the limit $(a_i/L_N) \ll 1$. The differential equation describing the wave has included the effects of non-uniformities in the electric and diamagnetic rotations as well as a finite Alfvén velocity. Accurate numerical results have been presented. Approximate analytic solutions have also been obtained using the local approximation and a Weber-Hermite approximation. The unstable modes found are ultimately due to the finite Larmor radius of the ions since when $a_i \to 0$ the wave becomes neutrally stable. Finite Larmor radius effects force ions to experience the electric fields and density gradients within the plasma differently than the electrons since the fields and gradients acting on an ion must be averaged over its Larmor radius. This causes the wave frequency to be less than the diamagnetic frequency over all or portions of the wave, thus upsetting the fine balance between electron Landau damping and destabilizing resonant particle effects. Any other effects within the plasma which enhance the resonant particle effects will destabilize the mode. It has been found that non-uniformities in the electric and diamagnetic rotations can provide the dominant contribution to the growth rate. The effect of non-uniform rotations

is further enhanced in lower density plasmas where terms involving $(C_A/C)^2$ are no longer negligible. Thus instabilities occuring in the presence of density gradients may in fact derive most of their energy from the velocity shear resulting from non-uniform rotations. This is thought to be the case for the collisional drift mode[15]. Since it was shown that an electric rotation opposing the diamagnetic rotation can almost eliminate velocity shear, imposing external radial electric fields on a plasma column may be an effective method for stabilizing the drift instability.

BIBLIOGRAPHY

(1) Krall, N.A., "Drift Waves", Advances in Plasma Physics, Vol.1, Interscience Publishers, Inc., New York 1968.

(2) Krall, N.A., Rosenbluth, M.N., "Low Frequency Stability of Nonuniform Plasmas", Physics of Fluids, 6, 254, (1963).

(3) Politzer, P.A., "Drift Instability in Collisionless Alkali Metal Plasmas", Ph.D. dissertation, Princeton University, (1969).

(4) Capjack, C.E., Stringer, T.E., "Drift Instability in the Presence of Nonuniform Radial Electric Fields", Canadian Journal of Physics, 49, 1630, (1971).

(5) Davidson, J.N., Kammash, T., "A Study of Plasma Stability in Sheared Magnetic Fields", Nuclear Fusion, 8, 203, (1968).

(6) Stringer, T.E., "Resistive, Inertial and Micro-Instabilities", Lectures delivered at NUFFIC International Summer Course on Waves and Instabilities in Plasmas, Breukelen, Netherlands, August 9-20, 1965.

(7) Meade, D.M., "Physical Mechanism for the Collisionless Drift Wave Instability", Physics of Fluids, 12, 947, (1969).

(8) Galeev, A., Oraevskii, V.N., Sagdeev, R.Z., "Universal Instability of an Inhomogeneous Plasma in a Magnetic Field", JETP, 17, 615, (1963).

(9) Stix, T.H., "The Theory of Plasma Waves", Chapter 7, McGraw-Hill Book Company, New York 1962.

(10) Little, P.F., Stott, P.E., "Low Frequency Drift Waves In A Q-Machine With Magnetic Shear", Bulletin of the American Physical Society, Series 11, Vol. 14, No. 11, Nov. 1969.

(11) Enriques, L., Levine, A.M., Righetti, G.B., "Experimental Study of the Effect of Radial Electric Fields on the Stability of a Magnetically Confined Plasma", Plasma Physics and Controlled Nuclear Fusion Research, Conference Proceedings Novosibirsk, Article CN-24/E-3, August 1 - 7, 1968.

(12) Nocentini, A., "Drift Waves in a Slightly Non-neutral Plasma" Journal of Plasma Physics, 3, 543, (1969).

(13) Fried, B.D., Conte, S.D., "The Plasma Dispersion Function", Academic Press, New York 1961.

(14) Rosenbluth, M.N., "Microinstabilities", Lectures presented at the Seminar on Plasma Phycics organized by and held at the International Centre for Theoretical Physics, Trieste, Oct. 5 - 31, 1964.

(15) Perkins, F.W., Jassby, D.L., "Velocity Shear and Low-Frequency Plasma Instabilities", Physics of Fluids, 14, 102, (1971).

(16) Schmidt, G., "Physics of High Temperature Plasmas", Chapter 8, Academic Press, New York 1966.

(17) Roos, B.W., "Analytic Functions and Distributions in Physics and Engineering", Chapter 7, John Wiley and Sons, Inc., New York 1969.

(18) Osborne, M.R., "A New Method for the Solution of Eigenvalue Problems", Computer Journal, 7, 228, (1964).

(19) Vedenov, A.A., Velikov, E.P., Sagdeev, R.Z., "Stability of Plasma", Uspekhi, 4, 332, (1961).

APPENDIX A

DERIVATION OF THE DIFFERENTIAL EQUATION DESCRIBING THE DRIFT INSTABILITY

The differential equation describing the drift instability in a non-uniform radial electric field is derived below by using the guiding centre approximation in cylindrical geometry[4]. Ion Landau damping, electron Landau damping and finite Larmor radius effects are included in this analysis. All assumptions are based on the experimental model discussed in sections 2.2 and 2.3. These assumptions are listed below:

i. A spacially uniform axial magnetic field $\vec{B} = B\hat{\epsilon}_z$ exists in the plasma.

ii. The velocities of the ions and electrons parallel to the magnetic field are described by Maxwellian distribution functions at the same uniform temperature T.

iii. The zero order radial electric field and density profiles are those given in section 2.3.

iv. The electron diamagnetic drift frequency (W_{EN}) and the electric drift frequency (W_E) are of the same order of magnitude.

v. All terms of order $(a_i/r)^3$ and higher are ignored since the region near the cylindrical axis is of no

interest (a_i is the ion Larmor radius and r is the distance from the cylindrical axis).

vi. A small electric field perturbation $\vec{E}_1$ is assumed to exist within the plasma at time t = 0. $\vec{E}_1$ has the following properties:

$$\vec{E}_1 = \vec{E}(r)\exp i(m\theta + K_{\parallel}z - Wt) \qquad (A.1)$$

$$\nabla \times \vec{E}_1 = 0 \quad \vec{E}_1 = -\nabla\phi_1$$

$$|\vec{E}_1| << |\vec{E}_o|$$

where

$\vec{E}_o$ = zero order radial electric field

m = azimuthal wave number

W = complex wave frequency

$K_{\parallel}$ = wave number parallel to the magnetic field

ϕ_1 = perturbed electric potential

vii. The wave frequency divided by the ion cylotron frequency (Ω_i) is assumed to be of the order $(a_i/L)^2$ where L is a characteristic length in the plasma (density or electric scale length). This assumption is based on the argument of section 2.1 which shows that $W \sim O(W_{EN})$. Terms of order $(a_i/L)^3$ and higher are ignored.

The differential equation describing the instability is derived in a cylindrical geometry where $\hat{\varepsilon}_r$, $\hat{\varepsilon}_\theta$, $\hat{\varepsilon}_z$ are unit vectors in the

r, θ and z directions respectively. Electromagnetic units are used throughout.

The zero order electric drift velocity perpendicular to the magnetic field is given for electrons or ions as:

$$\vec{V}_o = \frac{\vec{E}_o \times \vec{B}}{B^2} + \frac{1}{\Omega_{i,e} B} \frac{d\vec{E}_o}{dt} \qquad (A.2)$$

where "i,e" denotes ions or electrons respectively.

The effect of a finite ion Larmor radius (FLR) is obtained by averaging the electric field $\vec{E}_o$ seen by an ion over one gyration period. This is accomplished (to the order required) by applying the operator $\left[1 + 1/4 a_i^2 \nabla^2\right]$ to $\vec{E}_o$ in cylindrical co-ordinates[16]. Both the inertial and FLR effects of the electrons are ignored since the electron mass is much less than the ionic mass. The zero order drifts for electrons and ions are then given by:

$$\vec{V}_o^i = \left[1 + a_i^2/4(\nabla^2 - 1/r^2)\right](rW_E)\hat{\varepsilon}_\theta - \frac{rW_E^2}{\Omega_i}\hat{\varepsilon}_\theta$$

$$\vec{V}_o^e = (rW_E)\hat{\varepsilon}_\theta \qquad (A.3)$$

By the use of Poisson's equation, the zero order electron density (n_o^e) is obtained in terms of the zero order ion density (n_o^i).

$$n_o^e = n_o^i\left[1 + (C_A/C)^2 \frac{1}{r}\frac{(r^2 W_E)'}{\Omega_i}\right] \qquad (A.4)$$

where

$$C_A = \frac{B}{\left[4\pi M_i n_o^i\right]^{\frac{1}{2}}} = \text{Alfvén velocity}$$

C = velocity of light

$'$ = denotes differentiation with respect to r

The perturbed electric field $\vec{E}_1$ gives rise to a first order drift velocity perpendicular to $\vec{B}$ which is given for electrons or ions as:

$$\vec{V}_1 = \frac{\vec{E}_1 \times \vec{B}}{B^2} + \left[\frac{1}{\Omega_{i,e} B} \frac{d}{dt}(\vec{E}_o + \vec{E}_1)\right]_{[1]} \qquad (A.5)$$

where $[1]$ means that only first order terms in quantities such as $(a_i^2/r)^2$, (W/Ω_i) and $|\vec{E}_1|/|\vec{B}|$ are retained. The reason that $\vec{E}_o$, a zero order term is included in the expression for $\vec{V}_1$ is that "d/dt" is a convective derivative $\left[\partial/\partial t + (V_o+V_1)\cdot\nabla\right]$. Thus a term involving the zero order electric field when multiplied by a first order velocity will give rise to a term which is of the first order. Equation A.5 is evaluated using the finite Larmor radius operator for the ions. In calculating the first order electron drift velocity, FLR and inertial effects are ignored. The following expressions are then obtained for the first order ion and electron drifts:

$$\vec{V}_1^i = \left[1 - \frac{2W_E}{\Omega_i} + \frac{a_i^2}{4}(\nabla_1^2 - 1/r^2)\right] \frac{\vec{E}_1 \times \vec{B}}{B^2}$$

$$- \frac{i}{\Omega_i B}(W - mWI - ma_i^2\Omega_i/2r^2)\vec{E}_1 - \hat{\varepsilon}_r\, r(W_E/\Omega_i)' E_{1\theta}/B$$

$$\vec{V}_1^e = \frac{\vec{E}_1 \times \vec{B}}{B^2} \qquad (A.6)$$

where

$$WI = W_E(1-W_E/\Omega_i) + a_i^2/4(W_E'' + \frac{3}{r}W_E')$$

$$\nabla_1^2(\vec{\ }) = \hat{\varepsilon}_r\nabla^2(\ )_r + \hat{\varepsilon}_\theta\nabla^2(\ )_\theta + \hat{\varepsilon}_z\nabla^2(\ )_z$$

In order to calculate the first order particle density, an expression for the first order guiding centre density N_1 is required. This is obtained by using the equation of continuity for guiding centres.

$$\frac{\partial}{\partial t}(N_o+N_1) + (\vec{V}_o+\vec{V}_1)\cdot\nabla(N_o+N_1) + (N_o+N_1)\nabla\cdot(\vec{V}_o+\vec{V}_1) = 0 \qquad (A.7)$$

Using the assumptions that:

i. N_1 varies as exp $i(m\theta - K_{\parallel} z - Wt)$

ii. N_o and $\vec{V}_o$ are functions of r only with $\vec{V}_o$ in the $\hat{\varepsilon}_\theta$

iii. Second order terms $\vec{V}_1 \cdot \nabla N_1$, $N_1 \nabla \cdot \vec{V}_1$ can be ignored

the equation of continuity becomes:

$$-iWN_1 + (\vec{V}_o)_\theta \frac{imN_1}{r} + (\vec{V}_1)_r N_o' + N_o \nabla \cdot \vec{V}_1 = 0 \qquad (A.8)$$

When equations (A.3) and A.6) are substituted into equation (A.8), the following expressions for the perturbed ion and electron guiding centre densities are obtained:

$$N_1^i = \frac{-mN_o^{i\,\prime}}{(W-mWI)rB}\left[1 - \frac{2W_E}{\Omega_1} + \frac{a_i^2 \nabla_\perp^2}{4}\right]\phi_1 + \frac{\nabla_\perp \cdot N_o^i \nabla \phi_1}{\Omega_i B}$$

$$+ \frac{3mN_o^i \phi_1 W_E'}{(W-mW_E)rB\Omega_i} + \frac{im\phi_1 (N_o^i W_E')'}{(W-mWI)\Omega_i B} - \frac{iN_o^i}{(W-mWI)} \frac{d(V_1^i)_z}{dz}$$

$$N_1^e = \frac{-mN_o^{e\,\prime} \phi_1}{(W-mW_E)rB} - \frac{iN_o^e}{(W-mW_E)} \frac{d(V_1^e)_z}{dz} \qquad (A.9)$$

(Terms of the order (M_e/M_i) have been ignored.)

From Schmidt[16] the particle density can be expressed in terms of

the guiding centre density by applying the operator $\left[1 + 1/4a_i^2\nabla^2\right]$ to N_1. The perturbed ion and electron particle densities obtained from equation (A.9) are then given by:

$$en_1^i = \frac{e^2}{M_i\Omega_i^2 W_o r}\left\{\frac{1}{r}\frac{d}{dr}\frac{Sd\psi}{dr} + \frac{(1-m^2)S\psi}{r^3} + rW^2 n_o^{i\prime}\psi\right.$$

$$\left. - mW_o\Omega_i r n_o^{i\prime}\psi - i\Omega_i Brn_o^i \frac{d(\vec{V}_1^i)_z}{dz}\right\}$$

$$en_i^e = \frac{-e^2}{M_i\Omega_i^2 W_o r}\left\{rW_o\Omega_i mn_o^{e\prime} + i\Omega_i Brn_o^e \frac{d(\vec{V}_1^e)_z}{dz}\right\} \qquad \text{(A.10)}$$

where

e = electron charge

$W_o = W - mW_E$

$\psi = \phi_1/W_o r$

$S = W_o^2 r^3 n_o^i (1 - mW_\wedge/W_o)$

$W_\wedge$ = ion diamagnetic drift frequency (equation 2.24)

W_E = electric drift frequency (equation 2.23)

The final differential equation will be expressed in terms of the variable ψ for which physical interpretation will now be given.

The equation of motion for the guiding centres, ignoring inertial drifts, is given by:

$$\frac{d\vec{r}_g}{dt} = \frac{-\vec{E}}{B} .$$

Let $\vec{r}_g = \vec{r}_{go} + \vec{r}_{g1}$ and $\vec{E} = \vec{E}_o + \vec{E}_1$ where $\vec{r}_{g1}$ is the displacement of a guiding centre in a reference frame moving at the zero order drift velocity. Then the first order equation is:

$$(\partial/\partial t + \vec{V}_o \cdot \nabla)\vec{r}_{g1} = \frac{\nabla\phi_1}{B} \qquad (\vec{E}_1 = -\nabla\phi_1)$$

Using the approximation that $\vec{r}_{g1} \propto \hat{\varepsilon}_\theta \exp i(m\theta - Wt)$, the θ-component of this equation gives:

$$|\vec{r}_{g1}| = \frac{-m}{B} \frac{\phi_1}{W_o r} \propto \frac{\phi_1}{W_o r} = \psi$$

Thus ψ is proportional to the perturbed guiding centre displacement resulting from the perturbation ϕ_1.

The terms which still remain to be evaluated in equation (A.10) are $\frac{d(\vec{V}_1^i)_z}{dz}$ and $\frac{d(\vec{V}_1^e)_z}{dz}$. In this analysis it is assumed that the electron-ion collision frequency $\nu << \Omega_i$, Ω_e and that the ion Larmor radius is much smaller than the wavelength of the perturbation. Therefore, the drift approximation to the Vlasov equation[19] can be

used to calculate $\frac{d(\vec{V}_1)_z}{dz}$. This essentially replaces the particles by quasi-particles located at the guiding centres with magnetic moments μ. The distribution function f is now considered to be a function of the guiding centre position $\vec{r}_g$, the parallel velocity V_z and the magnetic moment μ. It is not considered a function of the guiding centre velocity since the guiding centre velocity is determined by $\vec{r}_g$ (equation A.12). In "drift-space", the Vlasov equation becomes:

$$\frac{df}{dt} = \frac{\partial f}{\partial t} + \nabla\vec{r}_g \frac{d\vec{r}_g}{dt} + \frac{\partial f}{\partial V_z} \frac{dV_z}{dt} + \frac{\partial f}{\partial \mu} \frac{d\mu}{dt} = 0 \qquad \text{(A.11)}$$

where $f = f(\vec{r}_g, V_z, \mu)$.

The equations of motion for the guiding centres are given by:

$$\frac{d\vec{r}_g}{dt} = \frac{\vec{B}V_z}{B} + \frac{(\vec{E}_o \times \vec{E}_1) \times \vec{B}}{B^2}$$

$$\frac{dV_z}{dt} = \frac{q(\vec{E}_1)_z}{M_{i,e}} \qquad q = \begin{matrix} e \text{ for ions} \\ -e \text{ for electrons} \end{matrix} \qquad \text{(A.12)}$$

$$\frac{d\mu}{dt} = 0 \quad \text{(consistent with the guiding centre approximation)}$$

Equation (A.11) is linearized by assuming $f = f_o + f_i$ where f_1 is

a small first order perturbation and f_o is a zero order Maxwellian given by:

$$f_o = n_o^{i,e}(r)\left[\frac{M_{i,e}}{2\pi kT}\right]^{1/2} \exp\left[\frac{-M_{i,e}V_z^2}{2kT}\right]$$

By substituting equations (A.12) into (A.11) the following expression is obtained for f_1:

$$f_1 = \frac{\frac{iq(\vec{E}_1)_z}{kT}\left[V_z - \frac{mW_D}{K_{\parallel}}\right]}{W - mW_E - K_{\parallel}V_z} f_o \qquad \text{(A.13)}$$

where

$$W_D = -\frac{n_o'}{n_o r}\frac{-kT}{qB} \quad \text{(electron or ion diamagnetic frequency)}$$

The macroscopic velocity parallel to $\vec{B}$ is obtained by averaging V_z over velocity space, that is:

$$(\vec{V}_1)_z = \frac{1}{n_o}\int_{-\infty}^{+\infty} f_1 V_z dV_z \quad \text{(Methods to evaluate this integral are given in reference 17)}$$

Thus the expressions obtained for $n_o^i \frac{d(\vec{V}_1^i)_z}{dz}$ and $n_o^e \frac{d(\vec{V}_1^e)_z}{dz}$ are:

$$n_o^e \frac{d(\vec{V}_1^e)_z}{dz} = \frac{-2e(\vec{E}_1)_z n_o^e}{M_e V_{TH}^{e\,2} K_{\shortparallel}} \left[1 + i\sqrt{\pi}\xi_e E(\xi_e)\right]\left[W_o - mW_{EN}\right]$$

(A.14)

$$n_o^i \frac{d(\vec{V}_1^i)_z}{dz} = \frac{+2e(\vec{E}_1)_z n_o^i}{M_i V_{TH}^{i\,2} K_{\shortparallel}} \left[1 + i\sqrt{\pi}\xi_i E(\xi_i)\right]\left[W_o - mW_{\hat{}}\right]$$

where

$V_{TH}^e = 2kT/M_e$ (electron thermal velocity)

$V_{TH}^i = 2kT/M_i$ (ion thermal velocity)

$\xi_e = W_o/K_{\shortparallel}V_{TH}^e$

$\xi_i = W_o/K_{\shortparallel}V_{TH}^i$

W_{EN} = electron diamagnetic frequency (Equation 2.26)

$$E(\xi) = \frac{2}{\sqrt{\pi}} \int_{-\infty}^{i\xi} e^{-s^2}\, ds\, e^{-\xi^2}$$

The final equation necessary for a self-consistent set is Poisson's equation.

$$-\nabla^2\phi_1 = 4\pi C^2(n_1^i - n_1^e)e \qquad (A.15)$$

By substituting the results of equations (A.1), (A.10) and (A.14) into (A.15), the following equation is obtained for ψ:

$$\frac{1}{r}\frac{d}{dr}\left(S_o \frac{d\psi}{dr}\right) + \psi\left[\frac{(1-m^2)S_o}{r^3} + rW^2 n_o^{i'} - (C_A/C)^2 K_{||}^2 n_o^i W_o^2 r^2\right]$$

$$- \psi\left[\frac{2r^2 W_o}{a_i^2}\left(n_o^e(W_o - mW_{EN})\ Z(W_o/K_{||}V_{TH}^e) + n_o^i(W_o - mW_\wedge)\ Z(W_o/K_{||}V_{TH}^i)\right)\right] = 0 \qquad (A.16)$$

where

$$S_o = W_o^2 r^3 n_o^i\left[1 + (C_A/C)^2 - mW_\wedge/W_o\right]$$

$$Z(\xi) = \left[1 + i\sqrt{\pi}\xi E(\xi)\right]$$

APPENDIX B

NUMERICAL METHOD OF SOLUTION

In this section the numerical method of solution for the equation discussed in chapter three will be given. The equation is of the form:

$$y''(r) - Q(r,W)y(r) = 0 \qquad \text{(B.1)}$$

where Q is an arbitrary function of r and the complex eigenvalue W. The assumptions that the mode is localized and that a perfectly conducting boundary exists at $r = r_p$ (plasma radius) gives rise to the following boundary conditions:

i. $y(0) = 0$

ii. $y(r_p) = 0$

The finite difference form of equation (B.1) is given by:

$$y_{n+1} - (2 + h^2 Q_n(W)) + y_{n-1} = 0 \qquad \text{(B.2)}$$

where

h = step size

$y_n = y(nh)$ with n an integer

$Q_n = Q(nh)$

If the variable N is taken to represent the number of internal node points, then N equations of the form given by (B.2) may be written:

$$
\begin{array}{ccccccc}
y_2 & - & (2+h^2Q_1)y_1 & + & y_o & = & 0 \\
y_3 & - & (2+h^2Q_2)y_2 & + & y_1 & = & 0 \\
\vdots & & \vdots & & \vdots & & \vdots \\
y_{N+1} & - & (2+h^2Q_N)y_N & + & y_{N-1} & = & 0
\end{array}
$$

with $y_o = y_{N+1} = 0$

The above equations may be expressed in matrix form as:

$$M(W)\underline{V} = 0 \qquad (B.3)$$

where

$$M(W) = \begin{bmatrix}
-(2+h^2Q_1(W)) & 1 & \cdots & 0 & 0 \\
1 & -(2+h^2Q_2(W)) & \ddots & \vdots & \vdots \\
0 & 1 & \ddots & 1 & 0 \\
\vdots & \vdots & & -(2+h^2Q_{N-1}(W)) & 1 \\
0 & 0 & \cdots\cdots & 1 & -(2+h^2Q_N(W))
\end{bmatrix}$$

$$\underline{V} = \begin{bmatrix} y_1 \\ y_2 \\ \vdots \\ y_N \end{bmatrix}$$

A method for solving this non-linear eigenvalue problem has been derived by M. Osborne[18]. The method has the following assumptions and properties:

1. The method is second order in that the error δ_{j+1} at the j+1 stage is proportional to δ_j^2 where δ_j is the error at the j^{th} stage.

2. The eigenvalues are assumed to be distinct.

3. Initial approximations are required. If

$$\underline{V}_{initial} = \underline{V}_{true} + \underline{q} \quad \text{where } ||\underline{q}|| < \delta$$

$$W_{initial} = W_{true} + \delta\eta$$

then the conditions for convergence are that:

   i. $\delta < 1/3$

   ii. $|\eta| < 1.5a$ where a is the minimum separation of the eigenvalues.

4. The iteration scheme used is given by:

$$M(W_i)\,\underline{V}_{i+1} = \frac{dM(W_i)}{dW}\,\frac{\underline{V}_i}{(\underline{V}_i)_p} \qquad (B.4)$$

$$W_{i+1} = W_i - 1/(\underline{V}_{i+1})_p$$

where p is the index of the component of maximum modulus in $\underline{V}$.

A computer program utilizing the above numerical method was written in Fortran IV. The initial eigenvectors were assumed to have components of the following form:

$$V_k = r^2(r-r_p)^2\left[\sin(n\pi r/r_p) + i\sin((n+1)\pi r/r_p)\right]$$

where

$r = kh$

$r_p = (N+1)h$

n = radial mode number

k = component index of $\underline{V}$ $(k=1,2...N)$

The initial values for W were chosen as $\text{Max}(mW_{EN} + mW_E)$. These initial values were systematically reduced until one of them converged to the desired radial mode. The frequencies, growth rates and eigenvectors were all calculated with a relative error less than .0002.